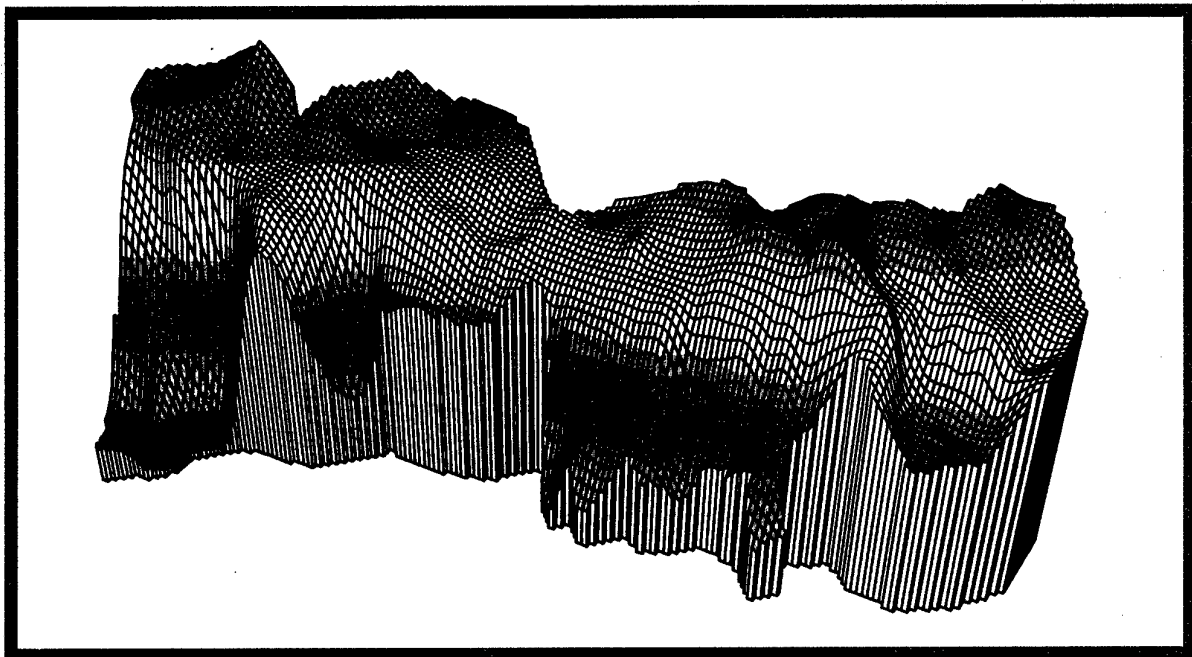


SACLANT UNDERSEA RESEARCH CENTRE REPORT



DISTRIBUTION STATEMENT A
Approved for Public Release
Distribution Unlimited

20010515 056

Analysis of towed array reverberation
data from 160 to 4000 Hz during Rapid
Response 97

Dale D. Ellis, John R. Preston, R. Hollett and
J. Sellschopp

The content of this document pertains to
work performed under Project 01-A of the
SACLANTCEN Programme of Work.
The document has been approved for
release by The Director, SACLANTCEN.



Jan L. Spoelstra
Director

intentionally blank page

Analysis of towed array reverberation data from 160 to 4000 Hz during Rapid Response 97

Dale D. Ellis, John R. Preston, R. Hollett and J. Sellschopp

Executive Summary: This report describes the reverberation and ambient noise experiments and analyses conducted onboard R/V *Alliance* during **Rapid Response 97**, a NATO MILOC Rapid Environmental Assessment (REA) exercise conducted in the Mediterranean during August and September 1997. It consisted of ASW (Anti-Submarine Warfare), MW (Mine Warfare) and AW (Amphibious Warfare) elements, in support of the follow-on NATO exercises **Dynamic Mix** and **Damsel Fair**. The areas surveyed were the Ionian Sea, Kyparissiakos Gulf off the west coast of Greece, the northern Adriatic Sea and Saros Gulf (west of Turkey).

Scientific and military personnel and ships and aircraft from institutions in Canada, France, Germany, Greece, Italy, the Netherlands, Turkey, the United Kingdom and the United States, participated in the data gathering and analysis.

The SACLANT Undersea Research Centre (SACLANTCEN) played a central role in the exercise by providing the Survey Director, an unclassified web site and data fusion centre for the measurements, as well as hosting the military personnel to provide classified products for **Dynamic Mix** and **Damsel Fair**. The Centre's research vessel R/V *Alliance* was deployed in the Ionian Sea and Kyparissiakos Gulf for more than 4 weeks, conducting oceanographic, bathymetric and acoustic measurements, as well as providing a large part of the Centre's data fusion effort.

The purpose of this collaborative experiment was to apply previously-developed research tools for reverberation analysis to the problem of rapid environmental assessment and to develop techniques useful to provide products in support of ASW operations.

The results illustrate the use of directional reverberation measurements as a useful remote sensing tool, for providing a quick map of an unknown area and directing higher-resolution measurements in potentially interesting areas.

intentionally blank page

Analysis of towed array reverberation data from 160 to 4000 Hz during Rapid Response 97

Dale D. Ellis^{*}, John R. Preston^{**}, R. Hollett and J. Sellschopp

Abstract: This report describes reverberation measurements made during the NATO MILOC Rapid Environmental Assessment exercise **Rapid Response 97**, August-September 1997. SUS charges were used as sources and data were received on two arrays towed by R/V *Alliance*: the 256-hydrophone Prakla array and the 32-hydrophone mid-frequency array. The arrays were towed on five-leg tracks at three locations: a deep water site in the Ionian Sea and two sites in Kyparissiakos Gulf, a small intermediate-depth basin off the west coast of Greece.

Reverberation data from the two arrays were analyzed in frequency bands from 160 Hz to 4000 Hz. Polar plots of the reverberation give a map of the prominent bottom-scattering features and provide a snapshot of the directional ambient noise field. Reverberation calculations were made using the Generic Sonar Model. A manual inversion procedure was used to estimate bottom loss and bottom backscattering. The model-data differences were used to produce scattering maps of the area. The polar plots and scattering maps indicated a number of scattering features not on the charts and identified a significant error in the charted position of an underwater escarpment to the south of Kyparissiakos Gulf. Follow-on swath mapping in two areas confirmed the results. The results illustrate the use of directional reverberation measurements as a useful remote sensing tool, for providing a rapid map of an unknown area and directing higher-resolution measurements in potentially interesting areas. The bottom loss and backscattering can be used in sonar models to provide improved performance predictions.

Keywords: Rapid environmental assessment – Rapid Response – reverberation data – inversion – scattering strengths – bottom loss – Ionian Sea – Kyparissiakos Gulf

^{*} Defence Research Establishment Atlantic, Dartmouth, Nova Scotia, Canada

^{**} Applied Research Laboratory, The Pennsylvania State University, State College, Pennsylvania, USA. Funded by Office of Naval Research

Contents

1. Introduction	1
2. Equipment, data acquisition and processing procedures	3
2.1. <i>Array towing pattern</i>	3
2.2. <i>Equipment</i>	4
2.3. <i>Acoustic data acquisition and analysis</i>	5
3. Site IA: Ionian Sea	9
3.1. <i>Propagation prediction</i>	9
3.2. <i>Long-range reverberation</i>	10
3.3. <i>Short-range reverberation</i>	11
3.4. <i>Difference map</i>	11
4. Site KD: Kyparissiakos Gulf area	12
4.1. <i>Long-range reverberation</i>	12
4.2. <i>Difference map</i>	13
4.3. <i>Higher frequency reverberation</i>	13
5. Site KH: Kyparissiakos Gulf area	15
5.1. <i>Long-range reverberation</i>	16
5.2. <i>Higher frequency reverberation</i>	16
5.3. <i>Difference map</i>	16
6. Bottom loss and bottom backscattering estimates	17
6.1. <i>Bottom loss and bottom backscatter functions</i>	17
6.2. <i>Model-data comparisons</i>	18
6.3. <i>Discussion</i>	20
7. High-resolution bathymetric mapping	21
8. Summary and discussion	22
8.1. <i>Site characterizations</i>	22
8.2. <i>Discussion</i>	25
9. Conclusions and recommendations	28
References	29
Annex A	31
Annex B	32
Annex C	35
Acknowledgements	36

Introduction

Rapid Response 97 was a NATO MILOC Rapid Environmental Assessment (REA) exercise conducted in the Mediterranean during August and September 1997. It consisted of ASW (Anti-Submarine Warfare), MW (Mine Warfare) and AW (Amphibious Warfare) elements, in support of the follow-on NATO exercises **Dynamic Mix** and **Damsel Fair**. The major areas were in the Ionian Sea and Kyparissiakos Gulf, off the west coast of Greece and the northern Adriatic Sea and Saros Gulf (Fig. 1).

Ships, aircraft and scientific and military personnel from Canada, France, Germany, Greece, Italy, the Netherlands, Turkey, the United Kingdom and the United States, participated in the data gathering and analysis.

The SACLANT Undersea Research Centre (SACLANTCEN) played a central role in the exercise by providing the Survey Director, an unclassified web site and the data fusion centre for the measurements, as well as hosting the military personnel to provide classified products for **Dynamic Mix** and **Damsel Fair**. The Centre's research vessel R/V *Alliance* was deployed in the Ionian Sea and Kyparissiakos Gulf for more than 4 weeks, conducting oceanographic, bathymetric and acoustic measurements, as well as providing a large part of the Centre's data fusion effort.

Measurements of reverberation and ambient noise were made at three sites: one deep-water site in the Ionian and two intermediate-depth sites in Kyparissiakos Gulf. The primary equipment for the reverberation measurements were SUS charges deployed from R/V *Alliance* and two horizontal towed line arrays: the 256 m multi-aperture Prakla low-frequency array and the 5.58 m aperture mid-frequency array. Additional reverberation measurements were made using the Towed Broadband Source and received on the mid-frequency array. Extensive oceanographic and transmission loss measurements were also made as part of the sea trial.

The reverberation measurements and analysis were part of a collaborative venture between scientists at SACLANTCEN, the Applied Research Laboratory of Pennsylvania State University and Defence Research Establishment Atlantic. The purpose of the venture was to apply previously developed reverberation analysis research tools to the problem of rapid environmental assessment (REA) and to develop techniques needed to provide products in support of ASW operations. An important part of the effort was to automate procedures to reduce delays in the displays and analysis. Problems in the automation system were expected

and were to be corrected if possible. Deficiencies and tools or topics needing further research, development and refinement were to be identified. Participation in the exercises enabled contribution to and benefit from, the developing concept of REA – a good opportunity for interaction between scientists and military officers. The interaction with researchers in different, but related, fields facilitated access to a rich data set, invaluable for testing and validating both scientific models and REA techniques.

The objectives of the trial were to demonstrate the technology and provide ASW products for the follow-on military exercises **Dynamic Mix** and **Damsel Fair**. Specific goals were:

- To use radar-like polar displays from impulsive sources (and pings) to display reverberation from a large area and to process the data in near real time (i.e., remote sensing).
- Using models such as the Generic Sonar Model, to predict directional reverberation on towed arrays in the areas of data collection; to use manual inversion procedures to obtain reasonable estimates of the bottom parameters; and to produce scattering maps of the model-data differences.
- To provide rapid turn around on acoustic characterization of the area: bottom loss, scattering strengths, false target zones, etc.; and to make these results available *via* the Web server.
- To extend the data analysis and software from low frequencies (less than 1500 Hz) to mid frequencies (up to 4000 Hz), using SACLANTCEN's new mid-frequency array.

Section 2 describes the experiment, the acquisition and the data processing. A key component is the BIMBO data acquisition and display software, which maps the processed reverberation onto a polar plot, resembling a radar display, which is superimposed on bathymetric contours. Sections 3 to 5 describe the measurements and analysis at the three sites, including the data, scattering maps and a discussion of the significant features, with reference to ambient noise, especially at mid-frequencies. The resolution of the polar plots was sufficient to identify a number of previously uncharted scattering features, a few of which were later surveyed with the swath mapping system (Section 7). Section 6 deals with the modelling, bottom loss estimation and scattering strengths. Section 8 deals with site characterizations and discussion of the results. The final section contains conclusions and recommendations.

Equipment, data acquisition and processing procedures

The R/V *Alliance* Information Management System (IMS) recorded ship track and weather information. Ship traffic is no longer automatically recorded by this system, but was monitored as part of the ambient noise analysis.

2.1 ARRAY TOWING PATTERN

Multiple tow directions are necessary to resolve the left-right ambiguity of the line array. A procedure developed by Wagstaff for ambient noise [1, 2] was adapted by Preston *et al.* [3, 4] for reverberation measurements. The reverberation measurements were carried out in conjunction with ambient noise measurements, as in previous REA and MILOC trials [5, 6]. Two arrays were deployed, towed at a speed of 4 to 6 kn. On each leg, the arrays were allowed to stabilize (about 20 min), after which 10 to 20 min of ambient noise were recorded. Several SUS charges were deployed (about 5 min apart) for reverberation measurements.

In previous trials, an irregular polygon (of 5 or more sides) was used, with a turn of 70° to 80° at the end of each leg. A typical side of the polygon was 4 to 6 n.mi –longer if there were problems with the recording equipment or defective SUS charges. Opposite sides of the polygon could be as much as 10 n.mi apart. While this may not be critical for ambient noise measurements in deep ocean areas, it does cause problems in confined shallow-water areas, as scattering features are illuminated from different ranges and angles. To alleviate this problem, a five-legged "petal" pattern was used, in which all five legs passed close to a common centre point (Fig. 2). The length of time for the recording is the same, but at least 15 min additional time is required on the turns as the average turning angle is 216° instead of 72°.

Figure 3 illustrates a towed array deployment for the reverberation and ambient noise experiments using SUS charges as sources. For the mid-frequency experiments with the towed broadband source, the Prakla array was recovered. Due to time constraints, the 5-sided petal pattern was replaced by a triangle, near the mid-point of the petal.

2.2 EQUIPMENT

SUS charges

SUS (Sound, Underwater Signal) charges (0.82 kg) were used as sound sources for the reverberation measurements. Two charges were dropped at 240 m and one at 18 m. To improve the stacking process, an attempt was made to drop one of the 240 m charges as close as possible to the centre point of the "petal". Typical times from drop to detonation were about 47 and 13 for the two depths. The spectral levels used for modelling are based on previous SACLANTCEN measurements (Annex A).

Prakla towed array

The Prakla towed array configuration consisted of a tow cable, two 50 m vibration isolation modules (VIMs), a 36 m high-speed digital link (HSDL), five acoustic sections of 64.5 m each, a 50 m tail VIM and a 20 m tail. The fore and aft acoustics sections are half populated with hydrophones and each contains a depth sensor and compass, separated by about 320 m. The acoustic section of the array was 254 m in length, consisting of 256 hydrophones with 3 nested sub-apertures of 128 hydrophones with spacings of 2.0 m, 1.0 m and 0.5 m. For a sound speed of 1500 m/s, these spacings correspond to design frequencies of 375, 750 and 1500 Hz respectively. For Site IA, the cable scope was 130 turns resulting in a distance of 1300 m from ship centre to acoustic centre of the array; the array depth varied between 245 and 335 m depending on the leg. For sites KD and KH, the cable scope was 50 turns or 710 m from the centre of R/V *Alliance* to the acoustic centre of the array; the array depth varied between 110 and 121 m.

Data from the 256 hydrophones of the towed array were digitized (12 bits) at 6000 Hz and recorded continuously on VLDS tapes as archival information for playbacks. A separate tape was used on each leg of the polygon; it includes both the ambient noise and reverberation measurements. Selected portions were also beamformed and recorded on optical disk using a Hewlett-Packard (HP) acquisition system (described below). To compensate for the low dynamic range, gain changes of 12 or 18 dB were made approximately 30 s after the direct acoustic arrival.

Mid-frequency array

The Mid-frequency array configuration for this experiment consisted of a tow cable, a 5 m HSDL, 75 m VIM, a 12 m acoustic section, a 50 m tail VIM and a 20 m tail. The acoustic section of the mid-frequency array included pressure and tilt sensors, a compass and 32

hydrophones at 0.18 m spacing. For a sound speed of 1500 m/s, this corresponds to a design frequency of 4167 Hz. The data acquisition uses the same equipment as the 64 hydrophone vertical array, developed at the Centre. The depth sensor (at the front of the array) was monitored at Sites KD and KH, where the depth varied from 73 to 78 m and 96 to 99 m. The log files contain the details, as well as the depth at Site IA.

Data from the 32 hydrophones were digitized (12 bits) at 12000 Hz and recorded on VLDS tapes. One tape was sufficient for each polygon; it includes both the ambient noise and reverberation measurements. Selected portions were also beamformed and recorded on optical disk using a Hewlett-Packard acquisition system (described below). To compensate for the low dynamic range, gain changes of 12 or 18 dB were commonly made 20 or 30 s after the direct acoustic arrival.

Towed broadband source

The towed broadband source contains several projectors which operate in different frequency bands. The ITC 1000 source has a resonance and peak power at about 3200 Hz; 3 dB points (measured outside the "fish") are at 2800 Hz and 4100 Hz. It has a dumbbell beam pattern forward and aft, with sidelobes of about -15 dB at "broadside".

On the mid-frequency runs, pings were transmitted every 2 min. Two LFM pulses and one CW pulse of about 1 duration were used, for a total of about 10 pings on each leg. Acquisition was on the WARP II system. The data could not be analyzed during the cruise. It has potential value, as the fathometer returns are not overloaded. As the beam response at 90° is poorly known and could be frequency dependent, a precise measure of the source level may not be possible.

Later in the trial, the broadband source was towed along some of the transmission loss tracks, with a 0.1 s LFM pulse (1100-1400 Hz) [7]. The near-vertical arrivals were recorded on the Prakla array along one track and the mid-frequency array along another track. When analyzed, they will provide valuable information on sediment layering.

2.3 ACOUSTIC DATA ACQUISITION AND ANALYSIS

The data acquisition and analysis procedure is summarized in Fig. 4. Details are presented below.

Time-domain beamformer

Using the ICS time-domain beamformer, beams for the Prakla array were formed using 128 hydrophones with a Hann window (128 non-zero elements) and steered at 125 angles, equally spaced in cosine of the beam angle from forward endfire to aft endfire. Three hydrophone channels were also recorded. Data were typically acquired for 3 min in deep water and 90 in shallow water, with a 10 to 30 s noise sample before the instant of the shot. On the 32-element mid-frequency array, a similar procedure was used; 33 beams (Hann-weighted and cosine-spaced) and 3 hydrophones were recorded for one minute.

Data acquisition programs

The new Hewlett-Packard workstation acquisition system was used to record the beam time series from the ICS beamformer on disk. As it does not have the real-time FFT capability needed for real-time operation, the beam time series were processed afterwards, using new versions of ISO266 and STACK (rewritten from the earlier WARP II real-time processing system).

The program STACK acquires the data in four frequency bands. For the low-frequency (2 m spacing) aperture, data in 50 Hz bands centred at 100, 160, 250 and 350 Hz were acquired. For the high frequency aperture (0.5 m spacing) the 50 Hz bands were centred at 630 Hz, 800 Hz, 1000 Hz and 1400 Hz. Then, 1024 point FFTs with non-overlapping Hann windows were used for spectral analysis, providing estimates of the beam and hydrophone time series at 0.17 s resolution (1024/6000). Energy is summed over the band of interest and divided by the bandwidth, to produce beam power normalized to a 1 Hz band. For the mid-frequency array the sampling rate was 12 kHz and the FFT size was 2048 points, again leading to a 0.17 s resolution. Four frequencies were recorded: 2000, 3000, 3500 and 4000 Hz; 150 Hz bandwidth was used for the two lower frequencies and 200 Hz bandwidth for the two upper frequencies.

STACK is run concurrently with a VAX-based auto-logging system to keep track of ship location, array heading, gain settings, etc., at the time of the charge drop to facilitate processing by the BIMBO display software.

ISO266 is similar to STACK, but obtains the data in third octave bands; (or, more precisely, one tenth decade bands with centre frequencies of $10^{n/10}$). Three frequency domains were processed: bands 14 to 28 (25 Hz to 630 Hz) with the 1 m spacing array, bands 27 to 32 (500 Hz to 1600 Hz) with the 0.5 m spacing and bands 31 to 36 (1250 to 4000 Hz) on the mid-frequency array (0.18 m spacing).

BIMBO display software

The BIMBO (Bistatic-Monostatic Beam Output) reverberation processing system was used to display the results from STACK. It was developed at SACLANTCEN [3, 4] for a VAX/VMS system and has been further developed at ARL/PSU where it runs on a DEC Alpha UNIX system. It preprocesses the STACK output using the DRAMR program and produces polar plots as a function of location, scalable on a Mercator projection so that a chart can be overlaid, enabling scattering features to be identified. Line plots of selected beams can be extracted using the HIL2PLOT program. UNIX command procedures, developed for **Rapid Response 96** and updated for this trial, greatly simplified the reverberation data processing. UNIRAS graphics [8] are used for the displays.

The polar plots with the depth contours are key to our reverberation analysis. The following is a brief description; see Preston et al. [3, 4] for details. If there are fewer than 128 beams, the beams are first mapped into 128 beams, using 1-D linear interpolation between beams. Each beam is considered as two radials on each side of the array heading (a 2-D approximation to the 3-D world). Using an average sound speed for the environment, each time sample is mapped into a range. Each range-bearing point is then mapped into an x-y point in Mercator projection. A UNIRAS 2-D interpolation routine then fills in the points on the rectangular display grid. The map is then output using a colour scale adjusted for the display desired.

For the stacked plots, the same procedure is repeated for the different headings (usually 5). Then the maps are "stacked", i.e., at each x-y point of the map the five (or so) values are averaged in dB.

The map contours are derived from a 5-minute gridded database based on DBDB5 [9] and contoured using a UNIRAS subroutine. The DBDB5 database often does not have enough fine-scale resolution, so an alternative map is sometimes manually overlaid to better evaluate returns from scattering features.

Acoustic modelling software

Our primary modelling program was the Generic Sonar Model (GSM) [10], developed at the US Naval Underwater Warfare Centre. We have had considerable success in using it to model reverberation. It is a comprehensive ray-based sonar model, which includes array beam patterns and computes surface, bottom and volume reverberation and fathometer returns. It has a bistatic capability, but as our source and receiver were in close proximity, GSM was used in monostatic mode. The source and receiver must be set at the same depth and an equivalent vertical beam pattern for a horizontal array is required. We used the average of the source and receiver depth for our computations and a small utility program to compute the effective vertical beam patterns [11] (averaged over the frequency band of interest).

Most of the of the inputs to GSM are standard and include:

- the measured sound speed profile (table)
- bottom loss (table)
- backscattering strength (table)
- Chapman-Harris surface scattering (wind speed)
- Marsh surface loss (wind speed)
- effective beam patterns (table)

A **Range Reference** of 1 m was used to correspond to our other units and an **Eigenray Tolerance** of 0.001 was used to ensure that sufficient steep angle rays were calculated at short ranges. For a source, GSM uses a pulse length and a (CW) source level. To model the explosives, we used a pulse length of 0.16 s (closely matched to processing time), with a source level correction of 8 dB [$-10 \log(0.16)$] added to the spectral levels given in Annex A. (Sometimes 0.17 s and +7.7 dB were used). The pulse length has little effect on the reverberation levels, but is an approximate match to the fathometer width and peak levels in the analyzed data.

Other useful models were: OASIS (a revised version of SAFARI [12]) (an ffp model), TRIMAIN [13] (a range-dependent ray trace) and RAM [14] (a high-angle parabolic equation code). These are all available over the Internet from OALIB (<http://www.njit.edu/oalib>).

Graphics programs included UNIRAS [8], MATLAB [15] and SAPLOT [16].

Site IA: Ionian Sea

Reverberation and ambient noise measurements were made on 25 August at Site IA, centred at location $36^{\circ} 17' N$ $16^{\circ} 47' E$. The water depth was about 3200 m. The sound speed was about 1540 m/s at the surface, with a weak surface layer to a depth of 23 m and a sound speed minimum of about 1510 m/s at a depth of 130 m. The Prakla and mid-frequency arrays were deployed to depths of 300 m and 70 m respectively; their distances behind the ship were roughly 1300 m and 500 m respectively. The array depths varied considerably, in spite of a constant tow speed of 4 kn with respect to the water, indicating fairly strong currents. There was a slight swell from the north. The bridge logs gave sea state 2 to 3 and wind speeds of 5 to 7 kn.

Three charges were dropped on each leg. Table 1 of Annex B summarizes the SUS drops for the polygon. Data from the Prakla array were recorded for 3 min and data from the mid-frequency array for 2 min.

3.1 PROPAGATION PREDICTION

Site IA is a flat area in the middle of the Ionian Basin, with no nearby scattering features visible on the charts. The major scattering features were expected to be on the Malta Escarpment, about 2.5 convergence zones to the west. Figure 5a shows ray paths for a 240 m source along a track from Site IA westward to the Malta escarpment. The plot shows rays for angles -7° to $+15^{\circ}$, made with the TRIMAIN program and plotted using a simple MATLAB interface. A single sound speed profile based on a CTD taken the day before the experiment was used in the calculations. Note the ray caustic which intersects the bottom at a range of about 105 km and depth of 2400 m. Other rays hit the bottom at slightly longer ranges and shallower depths. Strong backscattering is expected from these interactions. For a source at a different range, or a track along a different radial, the details will be different, but the general features will be the same.

Figure 5b shows a corresponding plot of the transmission loss at 350 Hz, made with the RAM parabolic equation code. The geoacoustic model, though not critical for this environment, was based on the bottom loss determined from the reverberation analysis. The figure also illustrates the sound speed profile.

3.2 LONG-RANGE REVERBERATION

The long-range reverberation was received on the SACLANTCEN Prakla array. The BIMBO software was used for much of the analysis and display. In the displays the explosive data have been averaged over a 50 Hz band, centred at the indicated frequency. Figure 6 shows a polar plot of the reverberation received on the beams of the towed array for the 350 Hz band, where the array has maximum resolution. Time has been mapped into range and beam angle into azimuth and the data are superimposed on the bathymetry. The arrow represents the array heading and the tail of the arrow indicates the array position at the time of the explosion: i.e., the array is at 36° 17' N 16° 47' E and is being towed northward. The black circle is the 60 marker (approximately 45 km).

There is high scattering near the array (red and orange colours), then the reverberation decays into the ambient noise (gray). The fathometers (multiple vertical bottom bounces) appear as concentric rings spaced about 4 apart; strictly speaking they should only appear on the broadside beam, but due to overloading at short times they appear on all beams. Many radials (usually in light blue) show high noise in the directions toward ships, indicating heavy shipping in this frequency band. (Note, however, that the number seems doubled, due to the left-right mirror-image effect of the towed array beam display). The ambient noise on the quiet beams is about 45 dB, corresponding to about 64 dB omni level background if no distinct ships were present.

The left-right ambiguity can be removed by combining the reverberation from the 240 m SUS charges received on five separate headings, as shown in the "stacked" plot in Fig. 7. The 5 black arrows indicate the array headings. Scattering can be seen (in orange) from the ridge to the west, as well as from the seamount to the south. There is scattering along the ridge to the west (roughly 15°45' E), often appearing at two ranges, as the ray plot of Fig. 5 suggested. The noise from many of the ships was too high to be completely suppressed by the stacking process and appears as blue radials. In these 5 two-minute "snapshots" over a 7 h period, there seems to be less shipping noise to the southeast.

A more complete analysis of the ambient noise field was performed on *Alliance* using the techniques of Refs. 1 and 2 and plotted on a map (Fig. 8) which shows the ship counts from a concurrent aircraft survey. The results confirm a large number of ships in the area, especially to the north and the directional noise roses quantify the impressions obtained from Figs. 6 and 7; for example at 350 Hz the beam levels in Fig. 7 of approximately 47 dB, plus the theoretical array directivity of about 19 dB, give 66 dB, close to the omni level of 68 dB in Fig. 8.

Figure 9 shows a stacked plot from a similar experiment during **Rapid Response 96**. It is similar to Fig. 7, but for a location near the base of the Malta escarpment. The different frequency, 630 Hz *versus* 350 Hz, will not affect things very much. The comparison illustrates the much stronger scattering due to the proximity to the steep slope; on single events, reverberation spikes occasionally jumped 30 dB above the background noise. The

comparison also illustrates the much-reduced distances between the array locations in the petal pattern (Fig. 7) compared to the 1996 polygon pattern (Fig. 9).

3.3 SHORT-RANGE REVERBERATION

At short ranges the bottom appears quite flat and featureless, which should be ideal for comparing the data with model predictions. Figure 10 shows a prediction using GSM and mapped with the same BIMBO polar display used for the data. The reverberation was calculated at 630 Hz for a selection of towed array beams: 0° (broadside), $\pm 10^\circ$, $\pm 30^\circ$, $\pm 45^\circ$, $\pm 60^\circ$, $\pm 65^\circ$, $\pm 70^\circ$, $\pm 75^\circ$, $\pm 80^\circ$ and 90° (endfire). The model assumes a uniform flat bottom and the corresponding fore and aft beams are identical. The bottom loss and bottom backscattering were adjusted to provide a reasonable fit to the average scattering (See Section 6). The noise level was set to 45 dB on each beam.

Although the bottom is uniform, the towed array beam patterns and propagation effects produce this typical deep-water pattern resembling a "crab" or "butterfly". At short times the near-broadside beams "see" the strong steep-angle bottom scattering (in magenta and red). The near-endfire beams see the bottom more weakly and at longer ranges (in blue). The endfire beam does not see the bottom at all for this environment; the short-range scattering shows up on the array sidelobes (assumed to be -35 dB).

Figure 11 shows a corresponding polar plot of the data in the 630 Hz band for all 125 beams of the towed array. As this is the 0.5 m spacing of the Prakla array, the beams are about twice as wide as at 350 Hz, so fewer shipping lines are visible than in Fig. 6. The plot is similar to the model prediction of Fig. 10, but contains radials from many ambient noise sources. The model data differences are shown in the next section.

3.4 DIFFERENCE MAP

Figure 12 shows a difference plot or scattering map for a single event at 630 Hz, on a smaller-scale map and with reduced spacing between colour levels. It gives an instantaneous picture of the overall quality of the fit, (which could undoubtedly be improved). The presence of numerous changes between the light blue and the light orange indicate best agreement. The differences beyond 5 n.mi are mainly due to the ambient noise appearing as radials, but a few scattering features appear (with left-right ambiguity); e.g., at $36^\circ 13' N$ $16^\circ 37' E$ (or the ambiguous location at $16^\circ 55' E$). Some features appear in front of and to one side of the array. There is a small overall fore-aft asymmetry in the differences. Two conditions could contribute to this: the slight increase in bathymetry to the north (see the contours on Fig. 7) and a slight forward tilt of the array during this polygon.

4

Site KD - Kyparissiakos Gulf area

Reverberation and ambient noise measurements were made in Kyparissiakos Gulf on 28 August near Site KD (37° 16' N and 21°19' E), with R/V *Alliance* towing the Prakla low-frequency array (for frequencies up to 1500 Hz) and the mid-frequency array (for frequencies up to 4 kHz). As at Site IA, the "petal" pattern of Fig. 2 was used, with SUS charges dropped at depths of 18 and 240 m while the ship was on 5 different headings. Table 2 of Annex B summarizes the SUS drops for the polygon. Data from the Prakla array were recorded for 2 minutes and data from the mid-frequency array for 1 minute.

The water depth was about 1200 m. The sound speed was about 1540 m/s at the surface, with a mixed surface layer to a depth about 20 m and a sound speed minimum of 1510 m/s at a depth of 90 m. The Prakla and mid-frequency arrays were deployed to depths of 115 m and 95 m respectively. Winds were light: the bridge logs gave sea states 3 to 4 and wind speeds of 7 to 15 kn.

The reverberation data analysis procedure was the same as that used at Site IA. The BIMBO reverberation analysis and display software was used to generate the polar displays.

Site KD is in an intermediate-depth basin, with the coast stretching from the north to the southeast, the islands of Strophades about 15 n.mi to the west and Zakinthos about 35 n.mi to the northwest. These features show up as prominent scatterers on the low-frequency array and the nearby ones show up on the mid-frequency array.

Ray plots show that the propagation is bottom dominated. Figure 13 shows a transmission loss plot in the direction of site KE near the coast to the southeast. The RAM model was used, with geoacoustic inputs consistent with the bottom losses obtained from our reverberation analysis of Section 6.

4.1 LONG-RANGE REVERBERATION

Figure 14 shows a stacked plot of the reverberation at 630 Hz, as received on the Prakla array at the 5 headings (black arrows). Long-range scattering can be seen from the island and seamount to the west, the island to the northwest, the coast from the north to the southeast and from near the rapid drop-off far to the southeast. Another sharp reflection appearing near 37° 03' N 21°33' E corresponds to an island. Note that for this figure we have overlaid a

bathymetry chart, having considerably more detail than the "DBDB5" contours presently available in BIMBO. The contours derived from a DBDB5 database show only a rising mound, which is actually two small islands (Strophades) near $37^{\circ}15' N 21^{\circ} E$; one chart [20] also showed a seamount at location $37^{\circ} 12' N 20^{\circ} 58' E$.

Even with the improved bathymetry of Fig. 14, the high scattering to the southeast (centred near $36^{\circ}48' N 21^{\circ}40' E$) appears to be closer to the coast than the escarpment indicated by the contours. A small area of swath mapping performed later (by R/V *Alliance* on 13 September) showed that, indeed, the map contours were in error by 1.5 to 2 n.mi. Section 7 shows this in more detail. Also shown in Section 7 are the results of a second bathymetric survey, conducted south of the Strophades; this time an additional seamount, not on any chart in our possession, was discovered.

4.2 DIFFERENCE MAP

Figure 15 shows a difference plot (data minus GSM model prediction) at 630 Hz for a single event with the Prakla array on a northerly heading. Note the much reduced colour scale for the difference plot compared with Fig. 14; also, there is left-right ambiguity, so the features show up twice. On this heading the reflections from the coast to the east and the island to the west, tend to be superimposed. The change in bottom slope about 8 n.mi in front of the array at $37^{\circ} 23' N$ causes this feature to stand out sharply. The longer-range scattering visible in Fig. 14 shows up strongly, as well as the noise from two nearby ships at bearings of 80° (or 275°) and 125° (or 230°). The model predictions are for a flat bottom with a Lambert scattering coefficient of -35 dB (quite low); the map thus provides an indication of the differences in scattering strength in the region near the array. There is of course the assumption that the bottom loss is uniform over the area; we expect some variation, but less variation than in the scattering, which is quite sensitive to the bottom slope. The reflection loss used for the modelling (Section 6) corresponds to a relatively hard bottom, possibly sand-silt. The normal-incidence bottom loss was estimated to be 10 dB at 630 Hz and at 3000 Hz.

4.3 HIGHER-FREQUENCY REVERBERATION

Figure 16 shows a plot of the scattering received on the mid-frequency array for a 150 Hz frequency band centred at 3 kHz. The scattering at short ranges drops off rapidly (red through dark blue) and is almost independent of azimuth. As this array is much shorter, the beams are much wider. Ships are strongly in evidence on two of the beams, at slightly different azimuths than in Fig. 15 as this event is about 6 min later. The noise is lower on the endfire beams, as they provide directivity against the surface reverberation.

Figure 17 shows a stacked plot for five events at 3000 Hz. Scattering from the coast to the southeast and from the island to the west appears above the background noise. The noise at long intervals is not completely isotropic, indicating residual directivity, probably due to shipping.

The ambient noise analysis shows a strongly directional noise field at 80 Hz, becoming less directional as the frequency increases to 1400 Hz. At low frequencies the noise is strongest to the NW and south; the eastern sector (N to SE) toward the coast is quiet compared to the western sector (N counterclockwise to SW). Even at 1400 Hz, however, there is about 15 dB of directionality, presumably due to shipping. The ambient noise analysis was not available for the mid-frequency array, though directivity would probably persist. Our stacked plots show directionality, though some of it may be due to distinct ships, which the ambient noise analysis tends to remove.

5

Site KH - Kyparissiakos Gulf area

Reverberation and ambient noise measurements were made outside Kyparissiakos Gulf on 30 August near Site KH (37° 25' N and 21°00' E), with R/V *Alliance* towing the Prakla low-frequency array (for frequencies up to 1500 Hz) and the mid-frequency array (for frequencies up to 4 kHz). As at Sites IA and KD, the "petal" pattern of Fig. 2 was used, with SUS charges dropped at depths of 18 and 240 m while the ship was on 5 different headings. Table 3 of Annex B summarizes the SUS drops for the polygon. Data from the Prakla array were recorded for 2 min and data from the mid-frequency array for 1 min.

The water depth was variable from about 1630-1780 m. The sound speed was about 1540 m/s at the surface, with a mixed surface layer about 20-22 m deep and a sound speed minimum near 1510 m/s at a depth of 77-80 m. The Prakla and mid-frequency arrays were deployed to depths of 115-130 m and 75 m respectively. Winds were stronger than at Site KD; over the duration of the measurements the sea state increased from about Beaufort wind force 6 to about force 8.

Site KH is at a "saddle point" lying between the small basin near Kyparissiakos Gulf and the deeper Ionian, with the coast stretching from the north to the southeast, two small islands (Strophades) about 5 n.mi to the south and a larger island (Zakinthos) about 15 n.mi to the northwest. These features show up as prominent scatterers on the reverberation data for R/V *Alliance* low frequency array and the closer ones show up on the R/V *Alliance* mid-frequency array.

The data analysis procedure was similar to that used at sites IA and KD, with the BIMBO reverberation analysis and display software was used to generate the polar displays. Some of the areas insonified by the SUS were the same as those insonified at Site KD, but from different angles.

Ray plots show that the propagation is bottom dominated. Figure 18 shows transmission loss in the northerly direction calculated using RAM, using geoacoustic parameters consistent with the bottom losses obtained from our reverberation analysis (Section 6). The sound speed profile is the same as for Site KD, but extended to 1800 m.

5.1 LONG-RANGE REVERBERATION

Figure 19 shows a polar plot of reverberation at 350 Hz for a single event with the low-frequency array on a southwesterly heading. The area gave many scattering highlights which could be taken for false targets. As there is a left-right ambiguity, the features show up twice, e.g., the "hot spot" displayed north of the array between the 250 and 500 m contours is really the rise to 1250 m east of the array. A closer look at this and other figures indicated good correlation with features found by the NAVOCEANO vessel USNS *Pathfinder* high-resolution swath survey during **Rapid Response 97**. One is a ridge about 5 n.mi northwest of the array at 37° 28' N and 20° 53' E. Another feature (a seamount) shows up at 37° 22' N and 20° 58' E. (It crosses the array heading arrow just above the 1250 m contour.) These features were not on any of the charts onboard R/V *Alliance*.

5.2 HIGHER-FREQUENCY REVERBERATION

Figure 20 shows a stacked plot of the scattering at 1400 Hz, received at low-frequency for five events. The scattering at short ranges is patchy and shows several returns to the south. (Note again that the contours, which are derived from a DBDB5 database, show only a rising seamount to the south, which is actually the island of Strophades and another small island, both near 37°15' N 21° E). Scattering is also visible from the coast to the northeast and from Zakinthos to the north. The ambient noise is fairly uniform in azimuth, but does indicate more noise to the west.

Figure 21 shows a polar plot at 3000 Hz. The noise is lowest toward shore; part of this is the forward endfire beam pattern which has vertical directivity, but the aft endfire beam has much higher noise. (The modulation on the forward beam is not yet identified – it has a 3 s period and is probably related to our ship or towed array motion in the 30 kn winds.)

The ambient noise analysis shows strong ambient noise directionality at low frequencies, with higher noise to the west (from NNW to SE). At 80 Hz there appears to be about 20 dB of directionality, reducing to less than 10 dB at 630 Hz and above. This is consistent with our stacked results at 1400 Hz in Fig. 20 and our fore-aft differences at 3000 Hz in Fig. 21.

5.3 DIFFERENCE MAP

Figure 22 shows the model-data difference plot or scattering map at 3 kHz. The model used a Lambert scattering strength of -27 dB, determined by our manual inversions (Section 6). The strong scattering feature to the east on the 1200 m contour also appears on the map from Site KD (Fig. 15), but to the south and east; i.e., the scattering is sensitive to relative slope rather than actual depths. Note that even at 3 kHz and in 30 kn winds, with a short array, scattering is visible from near the shore of Zakinthos.

6

Bottom loss and bottom backscattering estimates

6.1 BOTTOM LOSS AND BACKSCATTER FUNCTIONS

By comparison with model predictions, reverberation data can be used to extract estimates of bottom loss and scattering strength.

The bottom loss can be parameterized using the reflection coefficient between two homogeneous fluid half-spaces (the water and the seabed). The reflection coefficient R as a function of grazing angle θ (the angle with respect to the horizontal) is given by:

$$R(\theta) = \frac{\rho' c' \sin(\theta) - \rho c \sin(\theta')}{\rho' c' \sin(\theta) + \rho c \sin(\theta')} \quad (6-1)$$

where c and ρ are the sound speed and density in the water; c' and ρ' are the sound speed and density in the bottom and θ' is determined by Snell's law: $\cos(\theta') = c'/c \cos(\theta)$. (At steep angles θ' corresponds to the refracted ray in the bottom, but if c' is greater than c , then $\cos(\theta')$ will be imaginary at low angles of incidence). Attenuation is included as an imaginary part of the sound speed. The bottom loss (in dB) is given as $BL = -20 \log |R|$. Although the formula is expressed in terms of densities and sound speeds, the parameters that we found most useful in fitting the reverberation were the bottom loss at normal incidence, the critical angle (at which the bottom loss begins to rise steeply) and the seabed volume attenuation coefficient (which determines the loss at low grazing angles). More complex bottom loss *versus* grazing angle curves can be generated using models like OASIS and/or data from previous measurements.

The bottom backscattering uses a three-parameter fit to Lambert's rule at low angles plus a facet term at steep angles [17]:

$$S(\theta) = \mu \sin^2(\theta) + \frac{\nu}{\sin^4(\theta)} \exp\left(-\frac{\cot^2(\theta)}{2\sigma^2}\right), \quad (6-2)$$

where θ is the grazing angle and the facet term is characterized by a strength ν and a width σ . The backscattering strength (in dB) is given by $BS = 10 \log S$. The quantity $10 \log \mu$ (in dB) is commonly called the Lambert scattering coefficient, with Mackenzie's generic value of

-27 dB often being used for all frequencies and locations. The facet term is less commonly used in bottom scattering, though it corresponds to Chapman-Scott surface scattering at steep angles [18]. Some of the apparent facet strength and width, though modelled as scattering at the water-bottom interface, may in fact be due to volume scattering within the seabed.

6.2 MODEL-DATA COMPARISONS

Estimates of bottom loss and backscattering strength were made from the reverberation data using the Generic Sonar Model. Matching bottom parameters to fit the data results in an estimate of bottom loss *versus* grazing angle and scattering strength *versus* grazing angle.

Figure 23 compares the 630 Hz reverberation data (solid line) with a GSM model prediction (dashed line) at Site KH. The reverberation data are for the towed array on a northerly (350°) heading with the broadside beam looking east-west over a fairly flat portion of the seabed. Beam ambient noise for this event is shown as the horizontal dotted line. A 24 dB gain change took place 30 after the direct arrival; the small change in background noise indicates that the earlier levels probably included some bit noise of the A/D converter. The Generic Sonar Model assumes a flat bottom and the inputs include: the measured sound speed profile, wind speed, array beam patterns and source levels. The parameters for the bottom loss (solid line of Fig. 24) and backscattering (dotted line of Fig. 25) were adjusted to provide reasonable agreement between the data and model predictions.

The reflection loss used for the modelling corresponds to a relatively hard bottom. We used a bottom loss of 11 dB at normal incidence, a critical angle of 25° and an attenuation coefficient of 0.30 dB/m-kHz. Using Eq. (6-1) with $\rho = 1$ and $c = 1525$ m/s at the water-sediment interface gave $c' = 1683$ m/s and $\rho' = 1.62$, which are similar to a sand-silt bottom. This is a simple half-space model of the true bottom properties at Site KH, so one should not put a great deal of confidence in the physical parameters. However, we believe the reflection loss curve is a good starting point for more refined estimates. It seems to fit the short range data rather well, even in other look directions (not shown). It does not apply to the long-range feature scattering (between 22 and 30 in this example). The Lambert coefficient was -35 dB (quite low), the facet strength was -10 dB and the facet width was 10°.

A limited number of estimates of the bottom loss and backscattering strength have been made. In fitting the parameters for a site and frequency, we looked at data from one hydrophone and a selection of other beams: the broadside, endfire and the beam 30° from broadside seeming the most useful. Figures 24 and 25 illustrate the range of parameters found at Sites KD and KH.

Due to the low dynamic range of the recording system, much of the steep-angle scattering data is overloaded. Thus, at this site, our facet strength and width are not well determined.

The reflection loss at these sites is mainly sensitive to the steep angles of the bottom loss curve. In shallow water, the lower critical angles are more important.

At Site IA, the simple model of reflection loss was inadequate. Instead, we started with bottom loss curves from a nearby site [19]. The highest angle for which bottom loss was available was 78°. The multiple fathometer returns and steep angle scattering are quite sensitive to the bottom loss at vertical and near-vertical incidence. We tried adjusting the bottom loss curves at steep angles, but were unable to improve the agreement with the reverberation measurements. Our bottom-loss estimates at 90°, except for 160 Hz, appear to be a simple extension of the previously-measured bottom losses. Figure 26 shows the bottom losses used in fitting the reverberation at Site IA. The Lambert coefficients and facet coefficients are given in Table 6-1.

Table 6-1 *Initial bottom loss and backscattering estimates*

Site	Frequency (Hz)	Bottom Loss* (dB)	Lambert coefficient (dB)	Facet Strength (dB)	Facet Width (deg)
IA	160	16	-31	-15	15
IA	350	19	-32	-20	15
IA	630	16	-32	-20	15
r11**	800	13	-34	-15	12
IA	1400	15	-35	-20	15
IA	3000	13	-32	-15	7
KD	630	10	-35	-10	10
KD	3000	10	-27	-10	10
KH	630	11	-35	-10	10
KH	3000	11	-27	-10	10

* At normal incidence.

** Our estimate based on NAVOCEANO data from file rvbac018.dat on the SACLANTCEN WebServer.

Although there was insufficient information to be conclusive, our procedure was used to estimate the scattering strength from NAVOCEANO data posted on the **Rapid Response** Web server. For their site labelled r11 (near our Site IA), using our 630 Hz bottom loss and a Lambert coefficient of -35 dB provided a reasonable fit to their 800 Hz data. We aligned up the first fathometer returns from their 3 sonobuoys and used a water depth of 3400 m to match the fathometer returns. The agreement in scattering strength is excellent, showing the

utility of aircraft measurements in flat bottomed areas. In areas with features, their estimates are likely to be higher, since we can usually pick a beam that does not have any obvious feature scattering.

6.3 DISCUSSION

Reverberation depends in a complex manner on the bottom loss and scattering. The extracted scattering and bottom loss are therefore coupled, so that an error in the estimate of one of them will lead to an error in the estimate of the other. For our REA analysis, at most sites we have chosen to extract a minimal set of 6 parameters for each frequency (three geoacoustic parameters and 3 scattering parameters) which attempt to describe the bottom loss and scattering. In general these may be an inadequate physical description of the environment, due to gradients in the sub-bottom (which certainly exist for Site IA), or where a different scattering process (a different Lambert coefficient, or non-Lambert scattering) may dominate at low angles.

More work certainly needs to be done to refine the optimum parameter set; indeed, there is discussion as to whether the inversion process is unique. We feel the inversion is possible, but difficult to automate. It is important to ask the question: how much information is there in reverberation data? Reverberation data are intrinsically noisy due to the many paths and azimuths that contribute, as well as occasional scattering features. The many paths and the random scattering process mean that there is a lack of phase information which is a key component of matched-field inversions of controlled single-track transmission loss measurements. Even with high-quality transmission data, there can be ambiguities in the inverted parameters and one must be careful not to try to extract too many of them.

In the manual inversion procedure for this REA exercise our approach has been to start from the best possible *a priori* geological information, then make the smallest possible moves from that starting point in order to achieve reasonable agreement with the data from a number of reverberation measurements over the area.

Even with our reduced parameter set, our results are sometimes insensitive to some of the six parameters. For example in shallow water areas, where the reverberation is dominated by low-angle transmission, the facet scattering strength and width are poorly determined, but the bottom attenuation, critical angle and Lambert scattering coefficient are likely to be well determined. In the fairly deep water depths of this exercise, high-angle reverberation dominates, so the steep-angle bottom loss and scattering strength are likely to be better determined, although the towed-array beams towards endfire do aid in sampling the lower angles. However, the values we have extracted are well-matched to the environment and should be useful for active sonar predictions in a reasonably large area at frequencies from a few hundred hertz to several kilohertz.

7

High-resolution bathymetric mapping

Several hours of extra time for swath mapping by R/V *Alliance* became available near the end of the sea trial. Two of the anomalous features noted at site KD (Fig. 14) were mapped with the R/V *Alliance* swath mapping system and on both occasions interesting results were obtained.

Figure 27 shows the results of a mapping survey of the escarpment west of Pilos. The steep slope shown on existing charts is evident, but it is about 1.5 to 2 n.mi closer to shore.

Figure 28 shows the results of swath mapping to the south of Strophades. An uncharted seamount at 37° 12' N 21° 01' E, rising to approximately 40 m was mapped by R/V *Alliance*. The charts indicated a nominal bottom depth of 500 m in this area. One chart [20] showed a seamount rising to 20 m, about 2 n.mi to the north of this new seamount. There is a geological structure called the Strophades Ridge which extends southward from the island. We did not have time to confirm the seamount shown on the chart.

Some of the features noted at Site KH in Fig. 19 appear to be correlated with the swath bottom mapping conducted by the NAVOCEANO survey vessel USNS *Pathfinder*. However, these bottom features are more subtle than the features shown in Figs. 27 and 28.

8

Summary and discussion

This section begins with a summary of the work done during the sea trial and a brief summary of the acoustic characterizations of each site. It is followed by a discussion of the utility of directional reverberation analysis as a survey tool and some thoughts for further development of the concept.

8.1 SITE CHARACTERIZATIONS

Tables 8-1 to 8-3 summarize the acoustic characterizations of the three sites. Table 8-4 further summarizes the results and provides a condensed comparison of the two areas, the Ionian and Kyparissiakos Gulf. Table 8-5, derived from Table 6-1, compares the backscattering strengths in the two areas. These results were part of the "quick look" summary made at sea during the REA exercise.

Table 8-1 *Site characterization: Site IA*

- Deep ocean basin (~3200 m)
- Scattering from basin margins (at ~2.5 CZ's)
- Many ships visible on towed array beams
- Flat bottom at short ranges, with few nearby features
- Probable sub-bottom reflectors at lower frequencies, which could bias scattering-strength estimates
- Weak bottom scattering:
Lambert coefficients, -31 to -35 dB
- High bottom loss (frequency-dependent):
13 to 19 dB at normal incidence
in good agreement with previous lower-angle SACLANTCEN results
- Omni data from R/V *Alliance* in excellent agreement with NSODB aircraft data

Table 8-2 *Site Characterization: Site KD*

- Confined shallow-water basin (Kyparissiakos Gulf)
- No depth excess; strong bottom effects
- Scattering from shoreline, islands and features
Two uncharted features were found and later mapped
- Normal-incidence bottom loss 10-11 dB; consistent with sand-silt bottom
- Scattering weak at low frequency (-35 dB Lambert coefficient);
but normal at 3 kHz (-27 dB Lambert coefficient)
- Bottom features increase scattering by more than 10 dB on beams
- Directional ambient noise from shipping is very important;
(even at 3 kHz, one case showed 20 dB variation)

Table 8-3 *Site Characterization: Site KH*

- On ridge between Kyparissiakos Gulf and Ionian Basin
- Bottom loss and scattering strengths are much like Site KD
Lambert coefficients: -35 dB (630 Hz); -27 dB (3 kHz)
- Patchy scattering at low frequencies could be seen as false targets
- Uncharted features in reverberation displays were also identified in Pathfinder's swath maps made during the REA exercise
- Shipping noise is important: even at 3 kHz, with 30 kn of wind, the SACLANTCEN towed array showed that directional noise was present

Table 8-4 *Summary and comparison of site characterizations*

- Ionian Sea (~3200 m depth):
 - Transmission loss:* primarily via ducted low-loss paths
 - Bottom loss:* high, at steep angles
 - Backscattering:* low near Site IA
 - possibly some sub-bottom scattering
 - strong scattering from margins, 2.5 CZs distant
 - Directional noise:* many individual ships seen
- Kyparissiakos Gulf (up to 2000 m depth):
 - Transmission loss:* primarily via bottom-bounce paths
 - Bottom loss:* moderate
 - Backscattering:* low-to-moderate in flat areas
 - strong scattering from features and coast
 - Directional noise:* strong; even at 3 kHz many individual ships were seen

Table 8-5 Comparison of low-angle scattering strengths

Frequency(Hz)	Lambert coefficient (in dB)		
	Site IA	Site KD	Site KH
160/350	-32		
630	-32	-35	-35
1400	-35		
3000	-32	-27	-27

8.2 DISCUSSION

Usefulness of reverberation as a survey tool

Reverberation measurements contain all parts of the sonar equation: transmission loss (two-way propagation), reverberation (in azimuth, frequency and time) and ambient noise (from the background and from distinct ships). The processing also uses array gain and other signal processing techniques. There are also echos from features (or potentially even from real targets). In a very crude sense, the directional reverberation measurements provide "instantaneous" transmission loss measurements for an entire set of radials; the multiple types of scattering and the two-way propagation paths make interpretation difficult of course.

Although there are contributions from surface, volume, bottom and even sub-bottom reverberation, the dominant features appear to be determined by the bottom bathymetry. The polar plots, with the bathymetry superimposed, can be used to identify uncharted scattering features and are useful for directing more detailed surveys (as done on this trial and also in the 1996 **Rapid Response** exercise). The scattering maps provide a semi-quantitative map of the scattering strengths in an area. Even with 30 kn winds at 3 kHz, where surface noise and reverberation would be expected to dominate, bottom scattering features from the Island of Zakynthos were apparent.

The polar plots also provide a snapshot of the ambient noise directionality. The noisy beams provide a measure of the number of distinct sources and the quiet beams give a measure of the opportunities for detection. When stacked over a number of array headings, they provide a measure of the noise directionality.

Models are an essential part of attempting to quantify results and achieve a predictive capability. Our manual inversion procedure provides estimates of the bottom loss (which leads to better transmission loss predictions for both active and passive sonar), as well as estimates of the bottom scattering strength (for improved active sonar predictions).

The way ahead

There are a number of ways our analysis could be improved. Some of these are relatively straightforward, but others will require additional research.

The difference plots or scattering maps provide some measure of the scattering strength in an area; a relatively easy goal to achieve would be to obtain stacked difference maps.

The petal patterns were quite useful for reverberation analysis, in allowing the stacking method to more precisely locate features than with the previously-used polygon approach. We recommend using petal patterns for future reverberation stacking measurements.

A fast turn-around in the transfer of data from the acquisition system to the post processing system is needed, to obtain the scattering plots, checking that the gains are correct and that the system is working properly. A fast FFT box can provide this capability, but there may be other solutions.

The directional reverberation analysis is useful in identifying uncharted scattering features. To assist in interpreting and surveying known features, the best possible maps and charts should be available. The current "database" in BIMBO is DBDB5, which has very poor resolution for this type of survey. Based on our experience in this trial, the GEBCO [21] Mediterranean database is a strong candidate for incorporation into BIMBO. This is straightforward, but would require some effort.

The first few fathometer returns are quite strong, tending to clip the received signals at short intervals. The reverberation then drops quickly to near ambient noise levels. To alleviate this problem, we switched gains manually after 20 to 30 s. NAVOCEANO uses a set of 3 or 4 sonobuoys with up to 80 dB of padding to achieve an equivalent dynamic range. Neither of these solutions is satisfactory. A high dynamic range recording system is needed with automatic gain or 18 to 24-bit A/D conversion.

The manual extraction of bottom loss and scattering strength is a slow process. It is possible to automate this to some extent; Ellis and Gerstoft [22] used global inversion techniques for omni hydrophones in a fairly flat shallow-water area. It should be possible to extend this procedure, but would require considerable effort. An intermediate approach would be a semi-automated forward model and match approach.

Since the reverberation depends on both bottom loss and the bottom scattering, any error in one of them will have an effect on the extracted value of the other parameter. Also, there may be a better set of parameters that can be used to characterize the bottom loss and scattering; i.e., we essentially use a single parameter (the Lambert coefficient μ), to characterize all scattering at angles less than about 60° . Thus, more research into the inversion procedure is required and validation by direct measurement of scattering and bottom loss [23].

Modelling is an important component to any predictive capability. Scattering is sensitive to relative slope rather than actual bathymetry and strength and location depend on the angle of illumination. Models with both range and azimuthal dependence are needed, coupled with good databases. Although propagation models are relatively mature in this area, reverberation models are unsophisticated. Considerable research and development is required with models using empirical scattering functions such as Lambert's rule and with more physical models addressing the fundamental scattering problem.

At present, even though range-independent models are unable to predict details, they are very helpful in interpreting data. An important aspect of REA is the interpretation of the results; i.e., an expert can identify anomalous results quickly and re-direct detailed survey efforts; e.g., our swath mapping.

In the short term, many sonar models simply use Lambert's rule with a coefficient of -27 dB. We feel operational models should be able to accept a variable scattering coefficient (or different scattering function) and the databases should allow improved estimates to be incorporated.

9

Conclusions and recommendations

From our experience during this trial and the 1996 **Rapid Response** trial we feel that reverberation received on a towed array is a useful survey tool:

- Polar plots of the directional reverberation identified possible false targets and uncharted bottom features, which was useful for directing subsequent high-resolution surveys.
- By using model-data comparisons, quantitative estimates of bottom loss and backscattering strength were obtained, even in areas where there are a significant number of scattering features. These can be used for improved prediction for both passive and active sonar models.
- The technique is valid over a wide range of frequencies – during this trial, data from 160 Hz to 4000 Hz were analyzed.
- The reverberation not only samples the transmission loss and the scattering. It also provides a snapshot of the ambient noise. Thus a picture of the entire sonar equation (at all azimuths) is obtained.

Some recommendations for reverberation analysis in future REA exercises are:

- Use polar displays to provide a quick look at a large region and by overlaying the bottom bathymetry, determine areas of anomalous scattering.
- Investigate these anomalous areas in more detail with high-resolution systems, such as swath mapping or sub-bottom profiling.
- Improve the inversion procedure and make it more automated. Also validate it against direct measurements of scattering and bottom loss.
- Improve the models, striving for a predictive capability. Both range and azimuthal dependence are required, in conjunction with good bathymetric databases.
- Use the improved bottom loss and scattering estimates in AESS and other sonar models for improved sonar predictions.
- Improve the hardware where possible: e.g., high dynamic range receivers (18 to 24 bits), arrays which automatically resolve the left-right ambiguity and, of course, as much azimuthal resolution as possible in the beams.

References

- [1] Wagstaff, R. A. Iterative technique for ambient-noise horizontal-directionality estimation from towed line-array data, *Journal of the Acoustical Society of America*, **63**, 1978:863-869.
- [2] Wagstaff, R. A. Horizontal directivity estimation considering array tilt and noise field vertical structure, *Journal of the Acoustical Society of America*, **67**, 1980:1287-1294.
- [3] Preston, J. R., Akal, T., Berkson, J. Analysis of backscattering data in the Tyrrhenian Sea, *Journal of the Acoustical Society of America*, **87**, 1991:119-134.
- [4] Preston J. R., Kinney, W. Monostatic and bistatic reverberation using low-frequency linear FM pulses, *Journal of the Acoustical Society of America*, **93**, 1993:2549-2565.
- [5] Sellschopp, J. Environmental assessment prior to a naval exercise. *Naval Forces*, (6), 1997:25-27.
- [6] Nielsen, P., Jensen, F. B. Acoustic experiments and modelling results for the MILOC Rocky Road survey, SACLANTCEN SR-260. La Spezia, Italy, NATO SACLANT Undersea Research Centre, 1997.
- [7] Osler, J. Personal Communication, 1997.
- [8] UNIRAS users guide, Advanced Visual Systems Inc., Release 6.4a, Waltham MA, April 1994.
- [9] Eppert, H. C. *et al.*, Digital Bathymetric Database-5, NAVOCEANO, USA, July 1985.
- [10] Weinberg, H. The Generic Sonar Model, Naval Underwater Systems Center, New London, CT, USA, Technical Document 5971D, June 1985.
- [11] Ellis, D. D. Effective vertical beam patterns for ocean acoustic reverberation calculations, *IEEE Journal of Oceanic Engineering*, **16**, 1991:208-211.
- [12] Schmidt, H. Seismo-Acoustic Fast Field Algorithm for Range Independent environments - Users guide, SACLANTCEN Report SR-113. La Spezia, Italy, NATO SACLANT Undersea Research Centre, 1988.
- [13] Roberts, B. G. Jr. Horizontal-gradient acoustical ray-trace program TRIMAIN, Naval Research Laboratory, Washington, DC, USA, Report 7827, 1974.
- [14] Collins, M. D. A split-step Padé solution for the parabolic equation method, *Journal of the Acoustical Society of America*, **93**, 1993:1736-1742.
- [15] MATLAB reference guide, The Mathworks Inc., Natick, MA, USA, October 1992 (and later editions).
- [16] Young, C. A. SAPLOT Scientific graphic software user's manual, DREA, Dartmouth, NS, Canada, Technical Communication 91/307, December 1991.
- [17] Ellis, D. D., Crowe, D.V. Bistatic reverberation calculations using a three-dimensional scattering function, *Journal of the Acoustical Society of America*, **89**, 1991:2207-2214.
- [18] Chapman, R. P., Scott, H. D. "Surface backscattering strengths measured over an extended range of frequencies and grazing angles," *Journal of the Acoustical Society of America*, **36**, 1964:1735-1737.
- [19] Akal, T. Bottom-loss curves, Private communication, 1996.
- [20] Iónion SEA - Southern Part, Zákynthos Island to C. Tainaro, Map 22 INT 3418 (1:250,000), Hellenic Navy Hydrographic Service, Athens, Greece, December 1986.

- [21] GEBCO Digital Atlas & 1997 Supplement, British Oceanographic Data Centre, Proudman Oceanographic Laboratory, Bidston Observatory, Birkenhead, Merseyside UK, February 1997.
- [22] Ellis D. D., Gerstoft, P. Using inversion techniques to extract bottom scattering strengths and sound speeds from shallow-water reverberation data, in *3rd European Conference on Underwater Acoustics* (J. S. Papadakis, ed., FORTH, Heraklion, Crete, Greece) Vol. 1, 1996, pp. 557–562.
- [23] Holland, C. W., Neumann, P. Sub-bottom scattering: a modelling approach, *Journal of the Acoustical Society of America*, **104**, 1998:1363–1373.

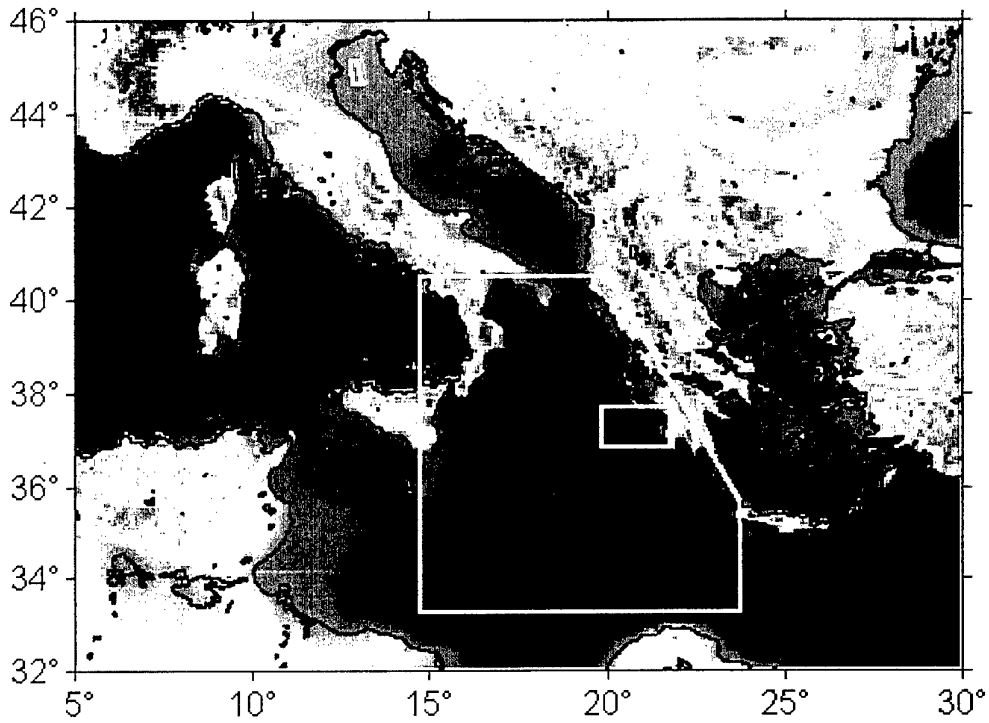


Figure 1 Chart of Rapid Response 97 REA exercise area, showing general bathymetry and sites of the reverberation measurements.

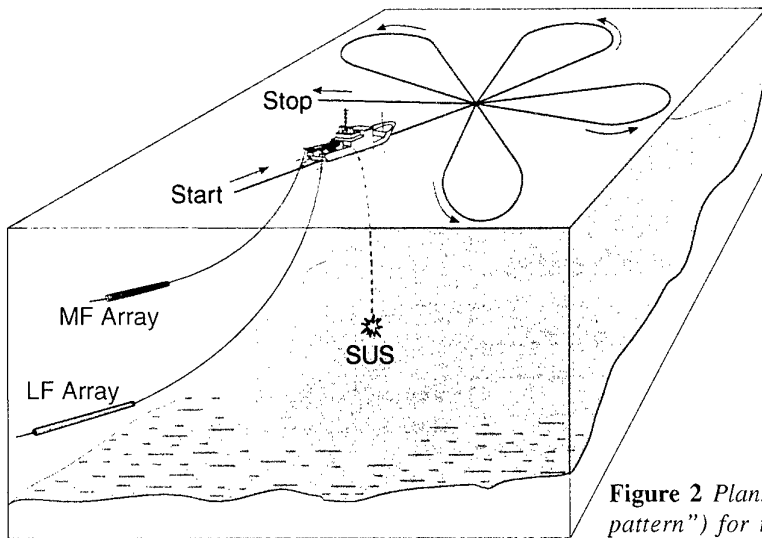


Figure 2 Planned ship track ("petal pattern") for the reverberation and ambient noise measurements.

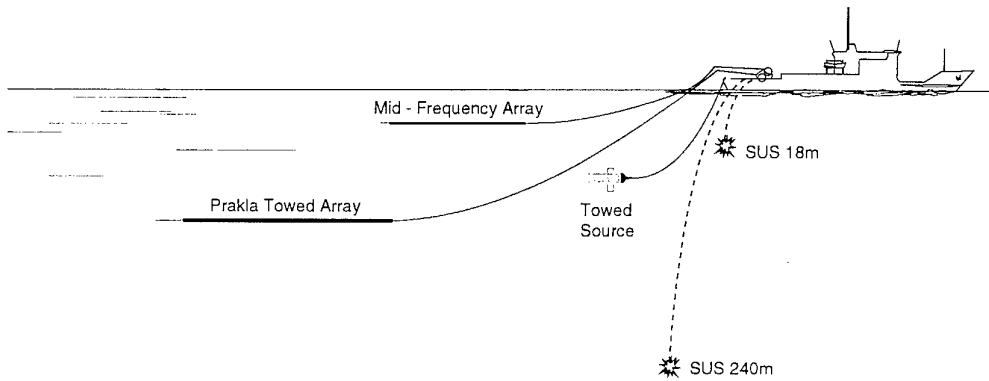


Figure 3 Schematic of towed array deployments for the reverberation and ambient noise experiments using SUS charges as sources. For the experiments with the mid-frequency source, the Prakla array was recovered.

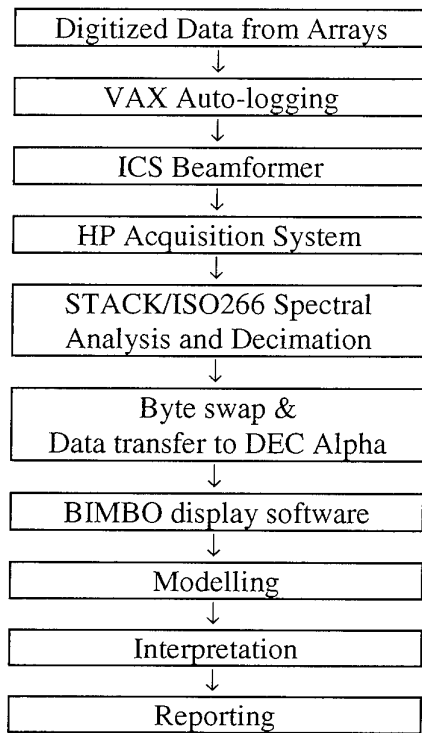


Figure 4 Schematic of the reverberation data acquisition and analysis procedure.

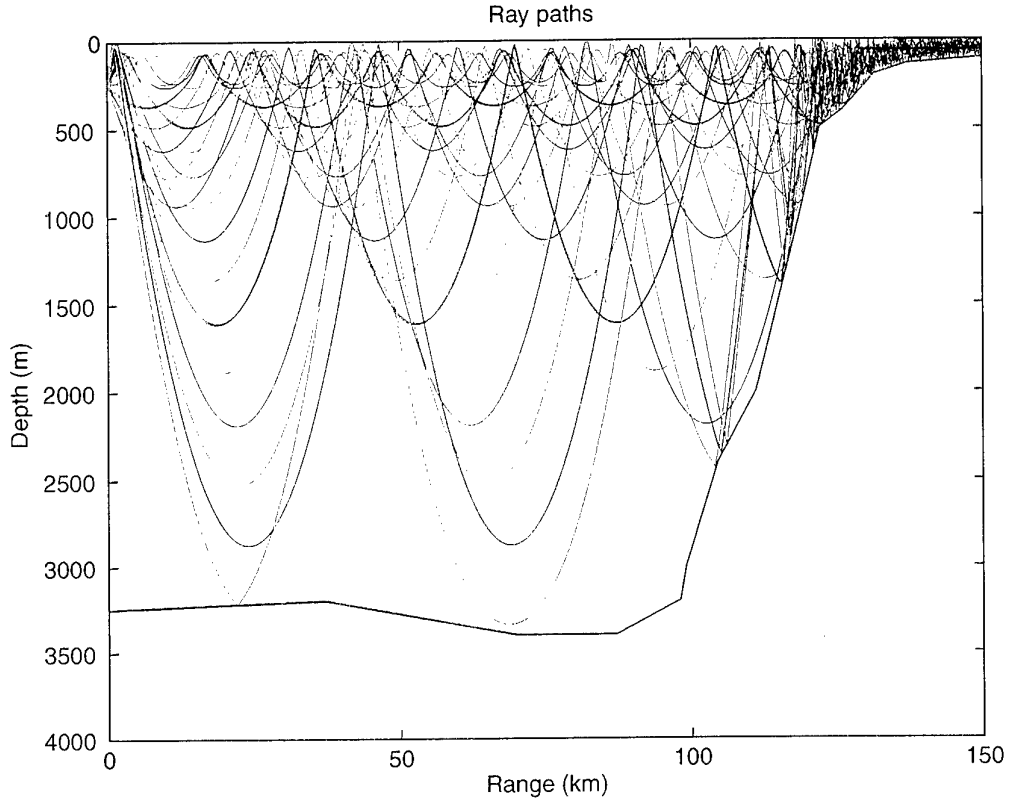


Figure 5a Ray plot of propagation paths for a 240 m source depth, along a track west from Site IA.

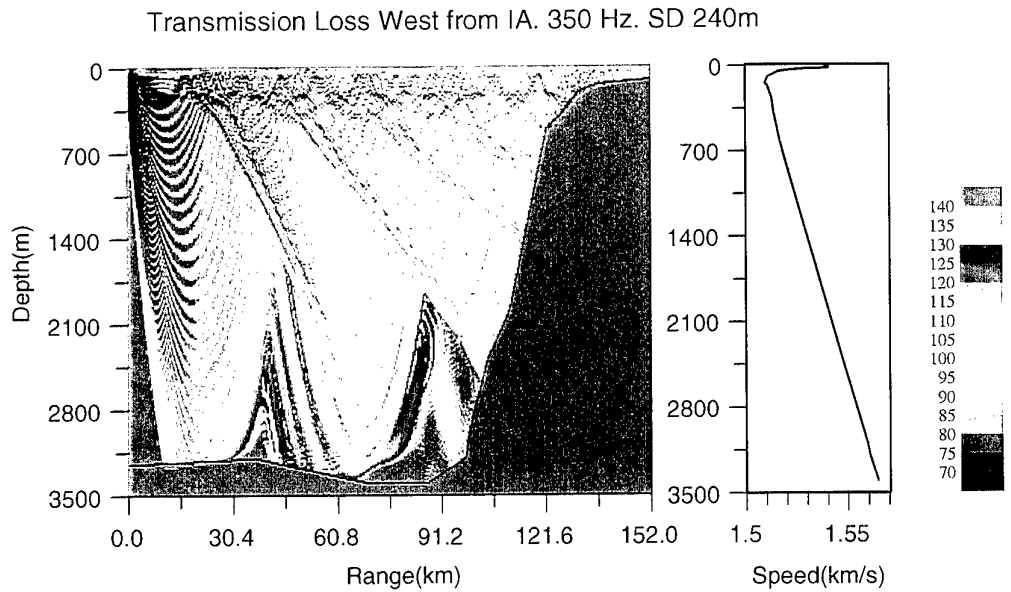


Figure 5b Transmission loss plot along the track shown in Figure 5a, using the RAM parabolic equation model. The sound speed profile is shown to the right.

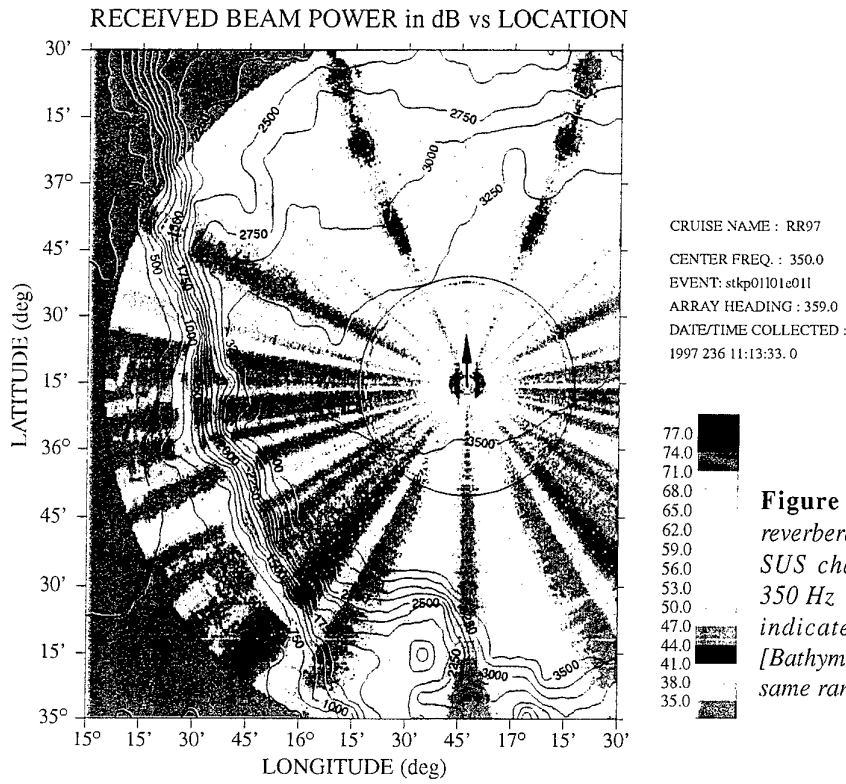


Figure 6 Polar plot of the reverberation from a single 240 m SUS charge at Site IA in the 350 Hz band. The black arrow indicates the array heading. [Bathymetry needs to be added; same range as Figure 7].

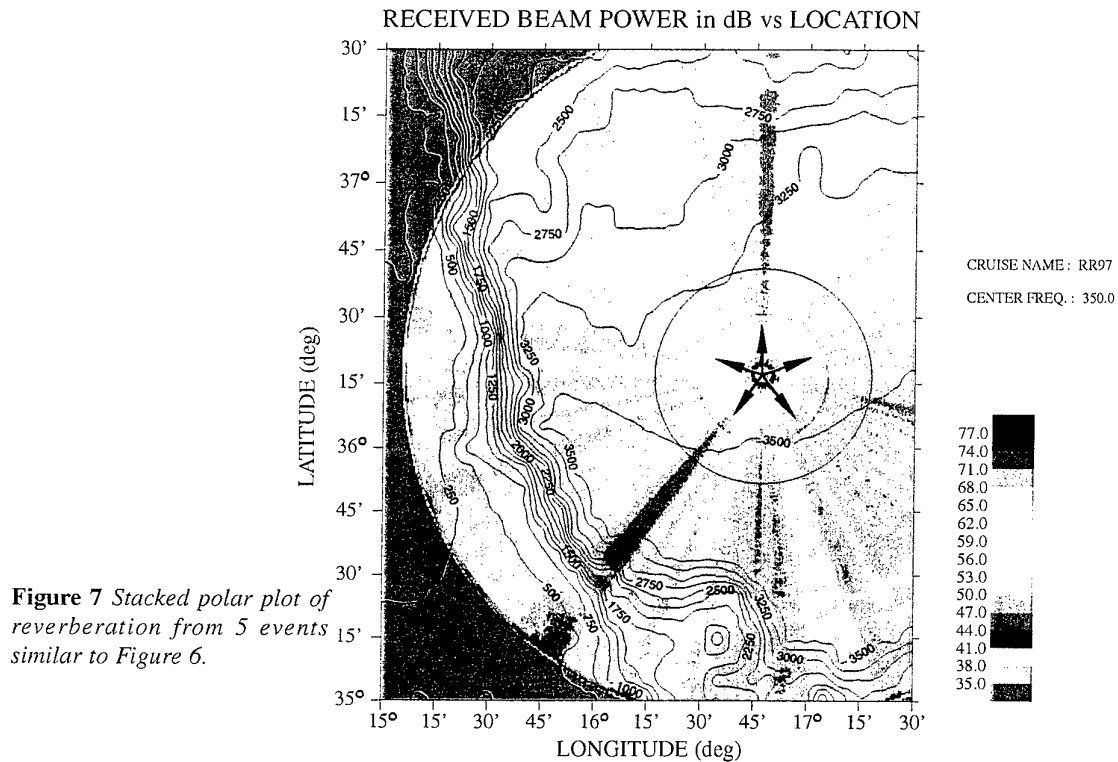


Figure 7 Stacked polar plot of reverberation from 5 events similar to Figure 6.

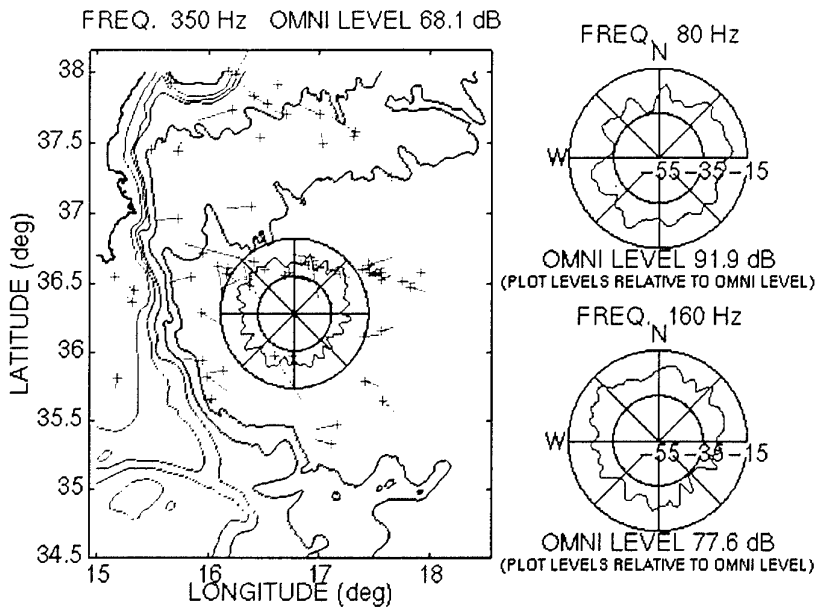


Figure 8 Reproduction of figure from the ambient noise analysis, showing locations of the ships noted in the aircraft survey and ambient noise directionality determined from towed-array measurements on R/V Alliance.

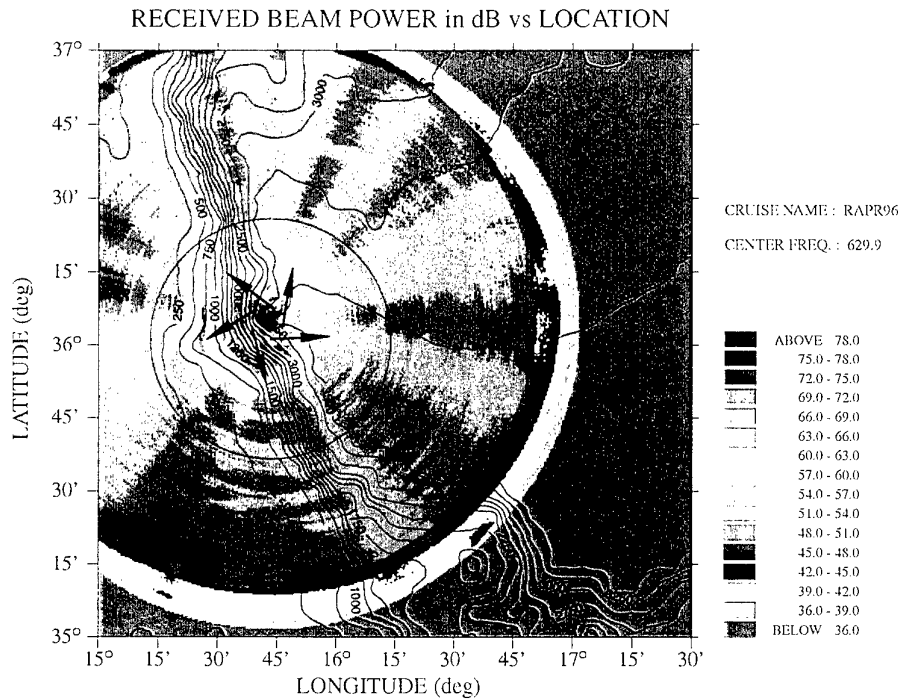


Figure 9 Stacked polar plot from Site AA of Rapid Response 96, near the base of the Malta escarpment. Compare this figure with Figure 7.

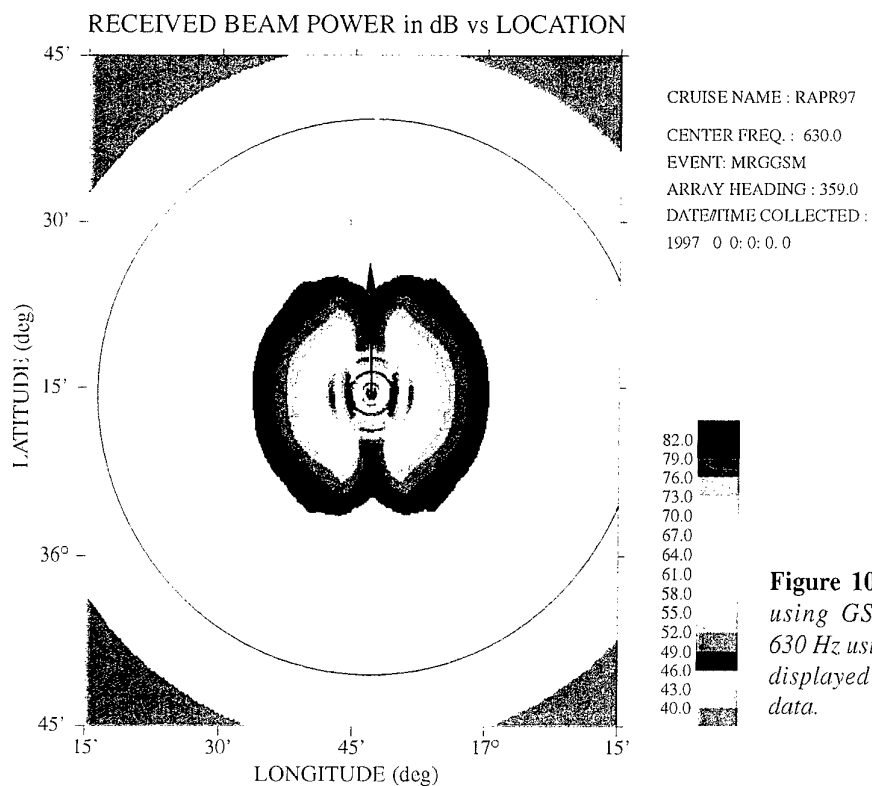


Figure 10 Predicted reverberation using GSM for a flat bottom at 630 Hz using 19 towed array beams, displayed in the same way as the data.

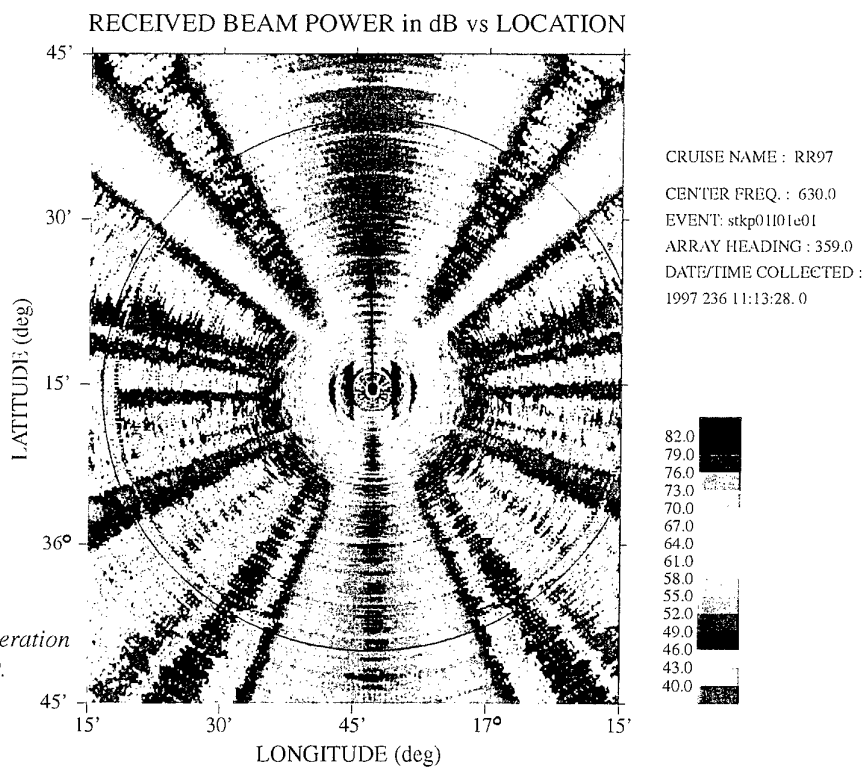


Figure 11 Measured reverberation corresponding to Figure 10.

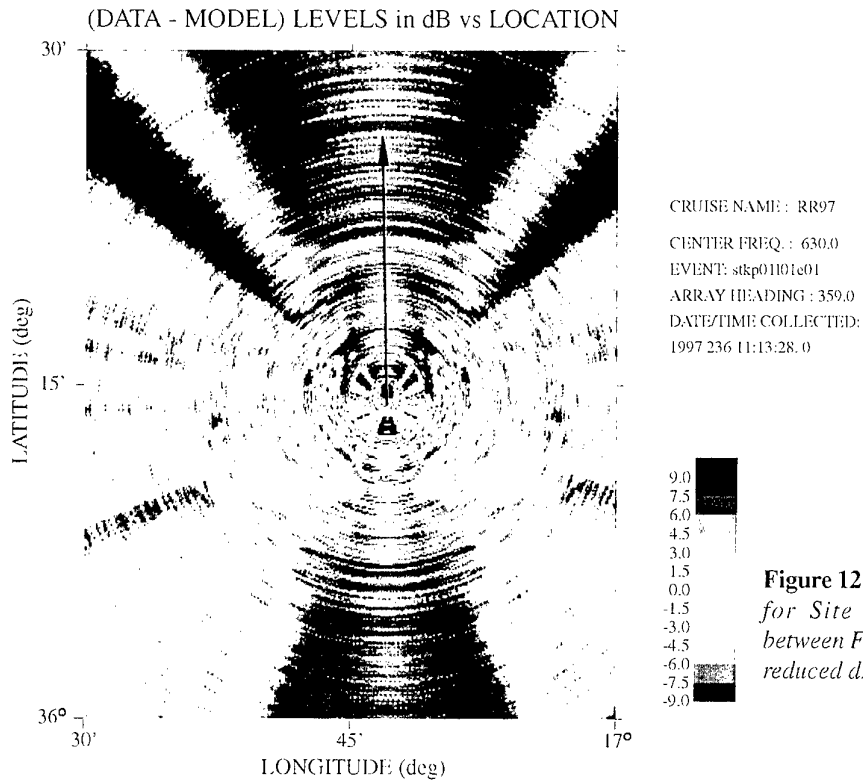


Figure 12 Scattering map at 630 Hz for Site IA: a difference plot between Figs. 10 and 11, on a much reduced dB scale.

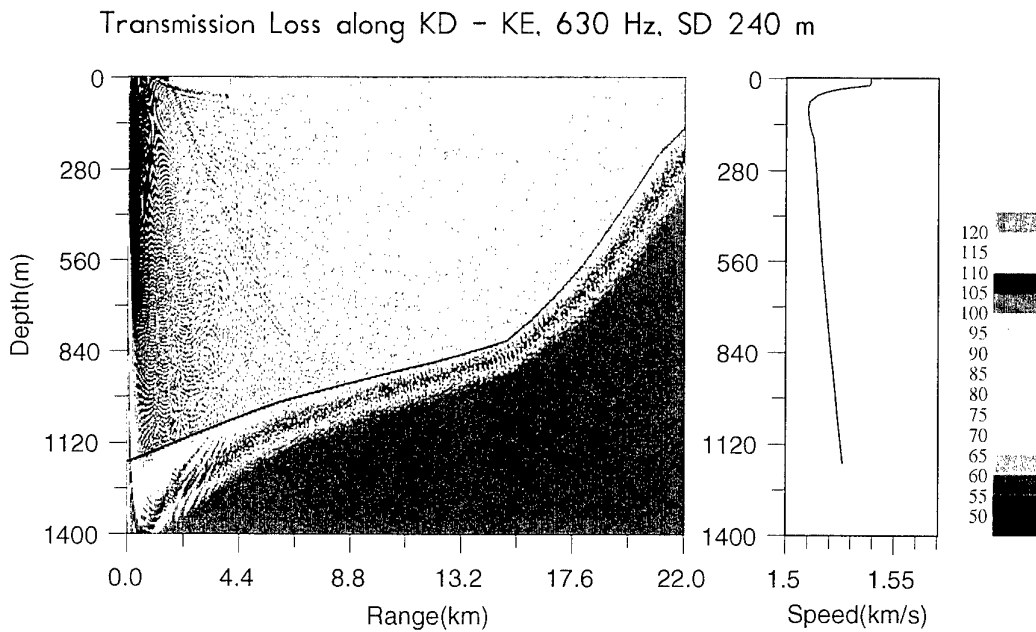


Figure 13 Sound speed profile and sample transmission loss plot at Site KD.

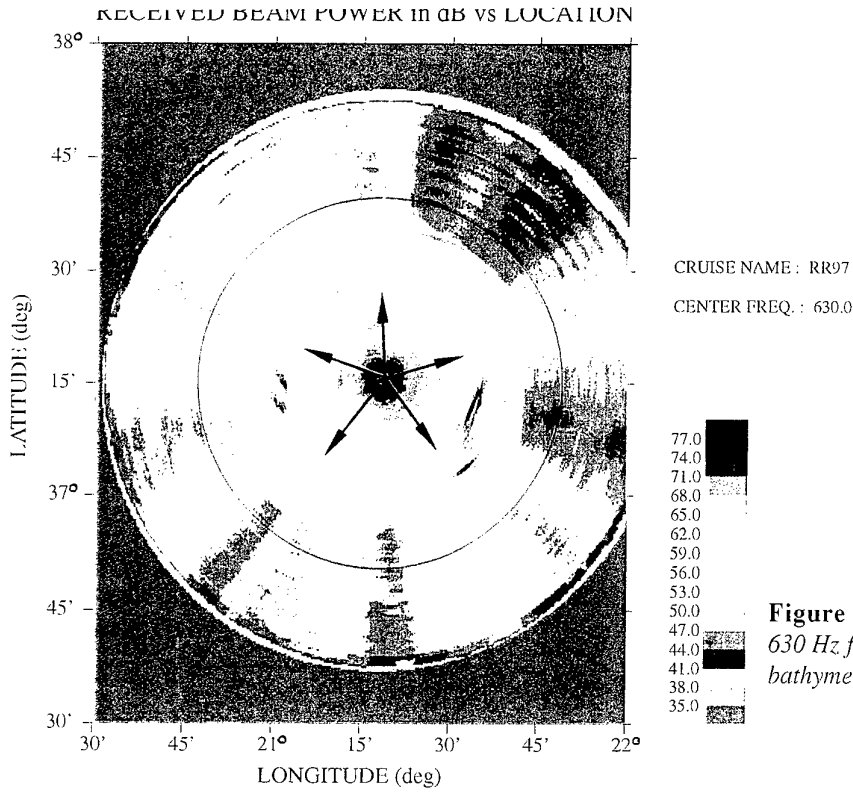


Figure 14 Stacked polar plot at 630 Hz for Site KD, using a detailed bathymetry overlay.

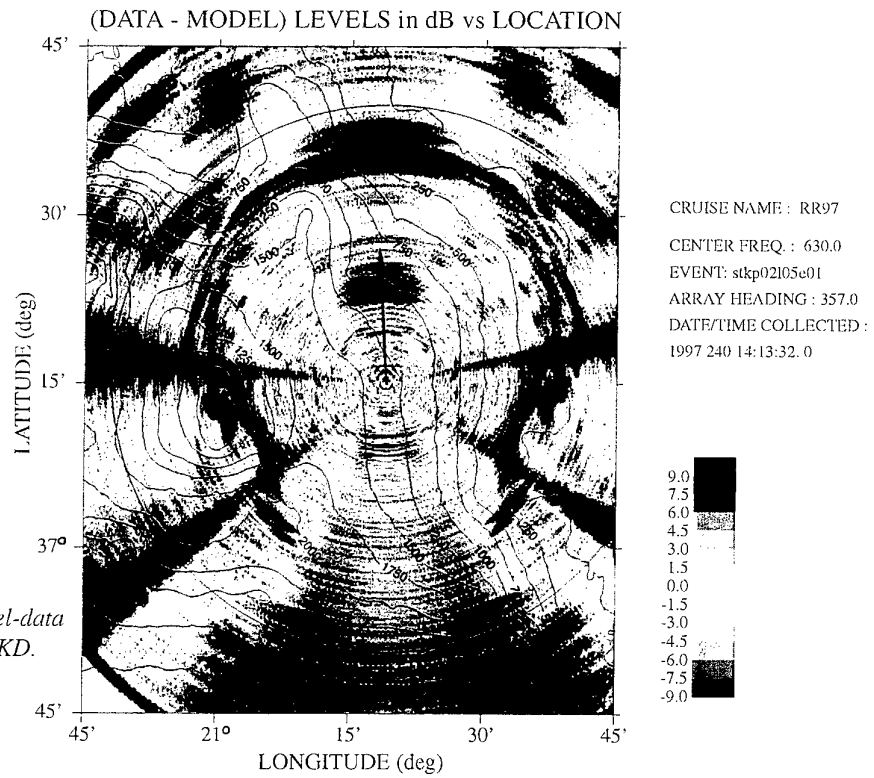


Figure 15 Scattering map (model-data differences) at 630 Hz for Site KD.

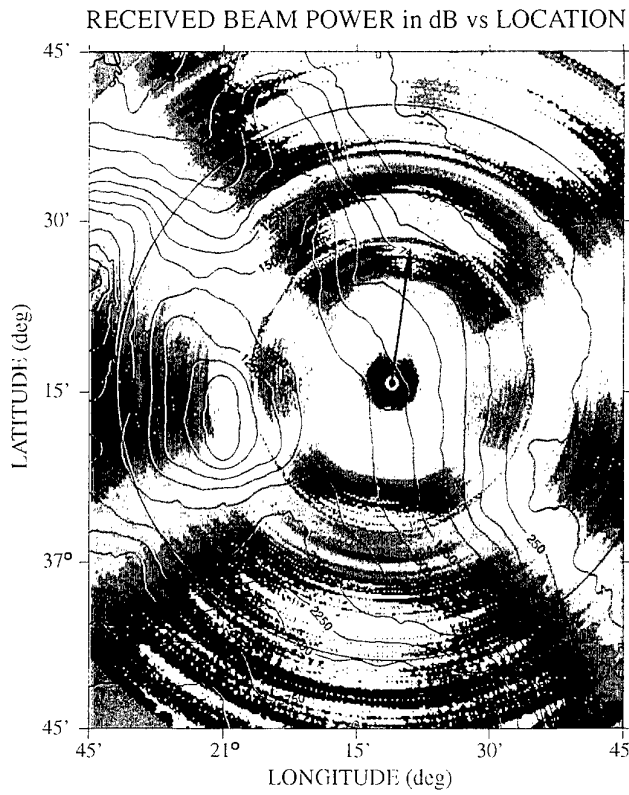


Figure 16 Polar plot at 3000 Hz for Site KD.

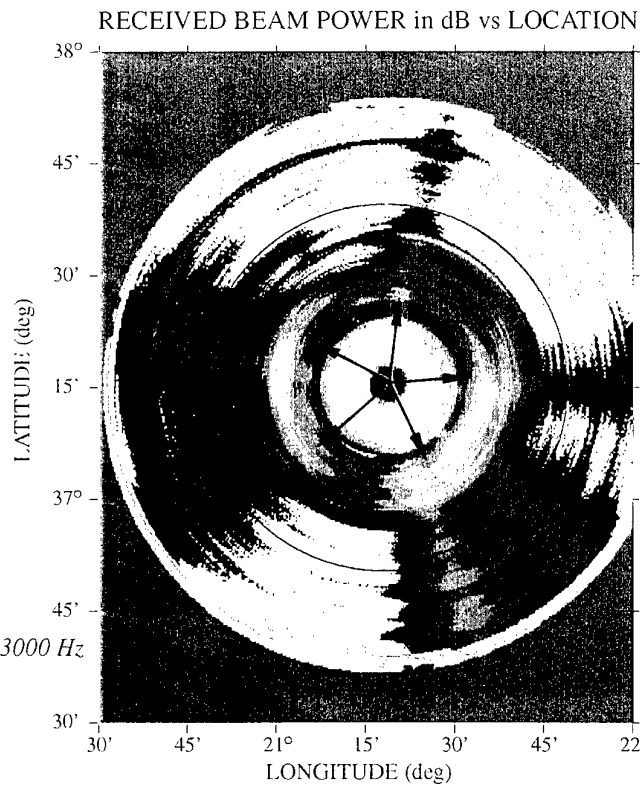


Figure 17 Stacked polar plot at 3000 Hz for Site KD.

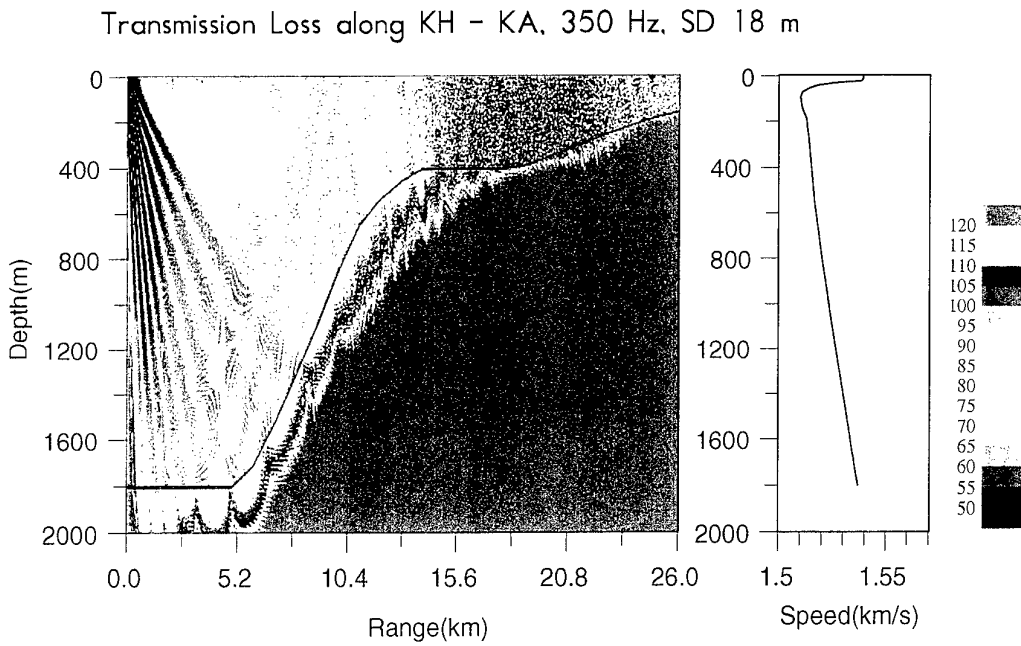


Figure 18 Sound speed profile and sample transmission loss plot at Site KH.

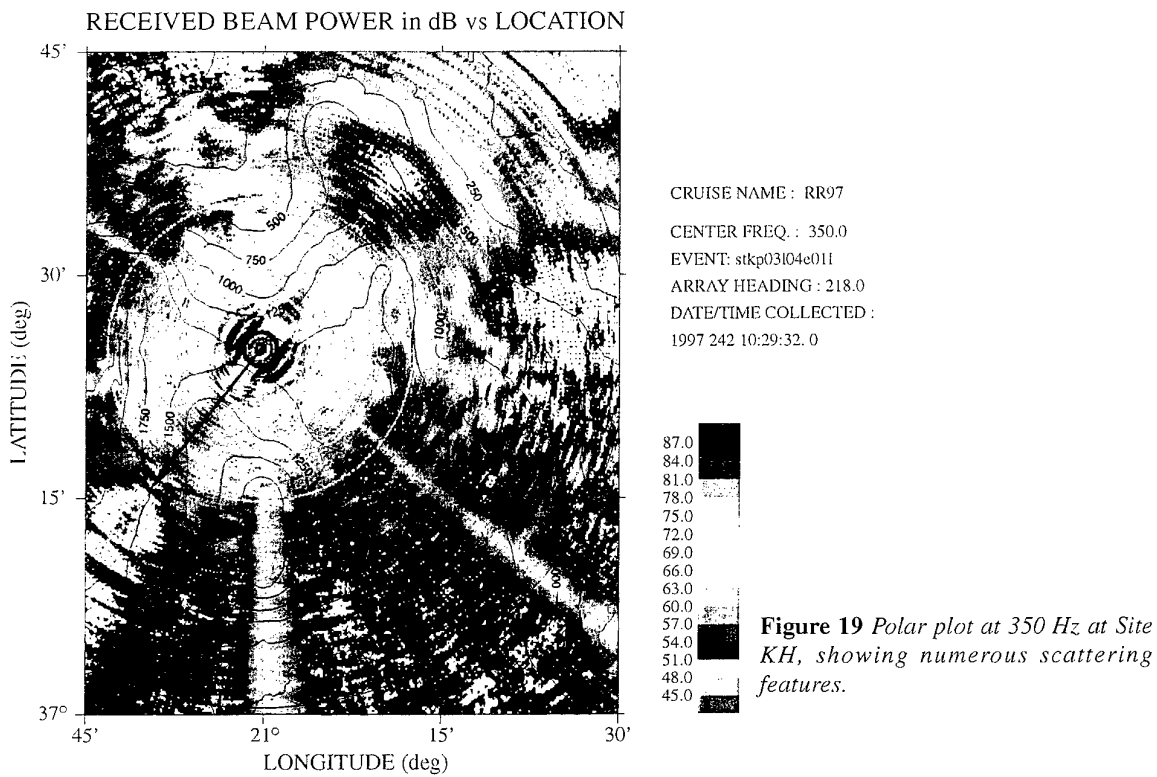


Figure 19 Polar plot at 350 Hz at Site KH, showing numerous scattering features.

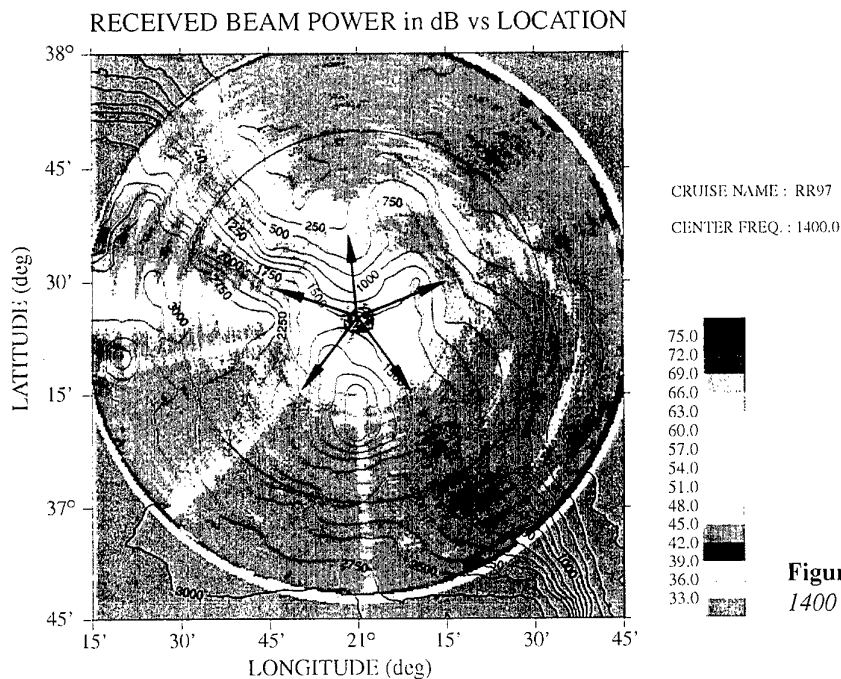


Figure 20 Stacked polar plot at 1400 Hz at Site KH.

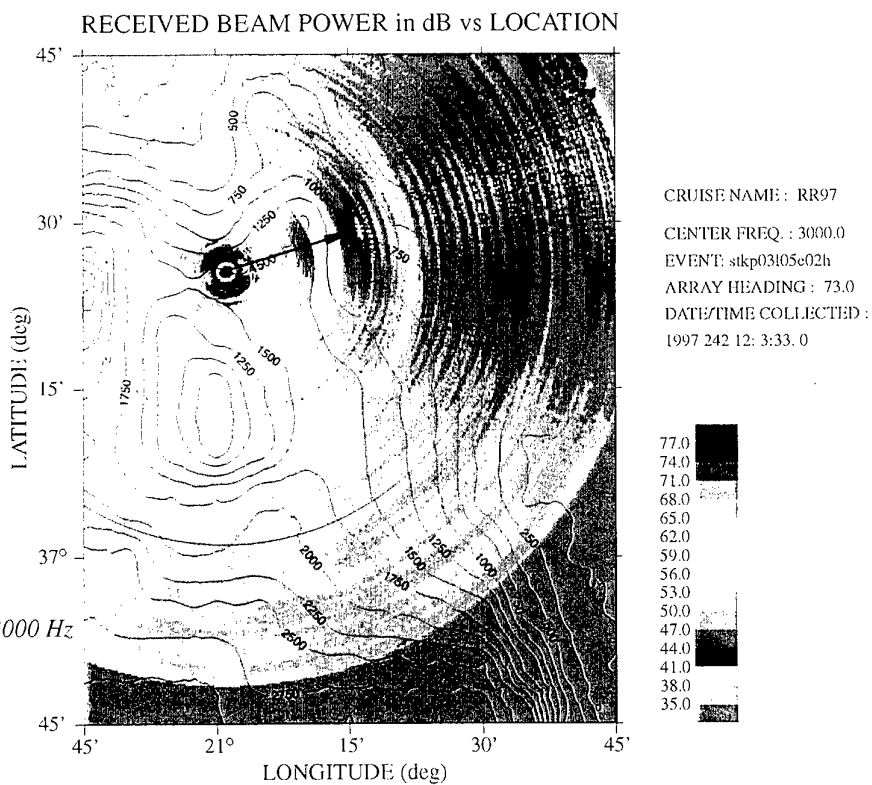


Figure 21 Polar plot at 3000 Hz at Site KH.

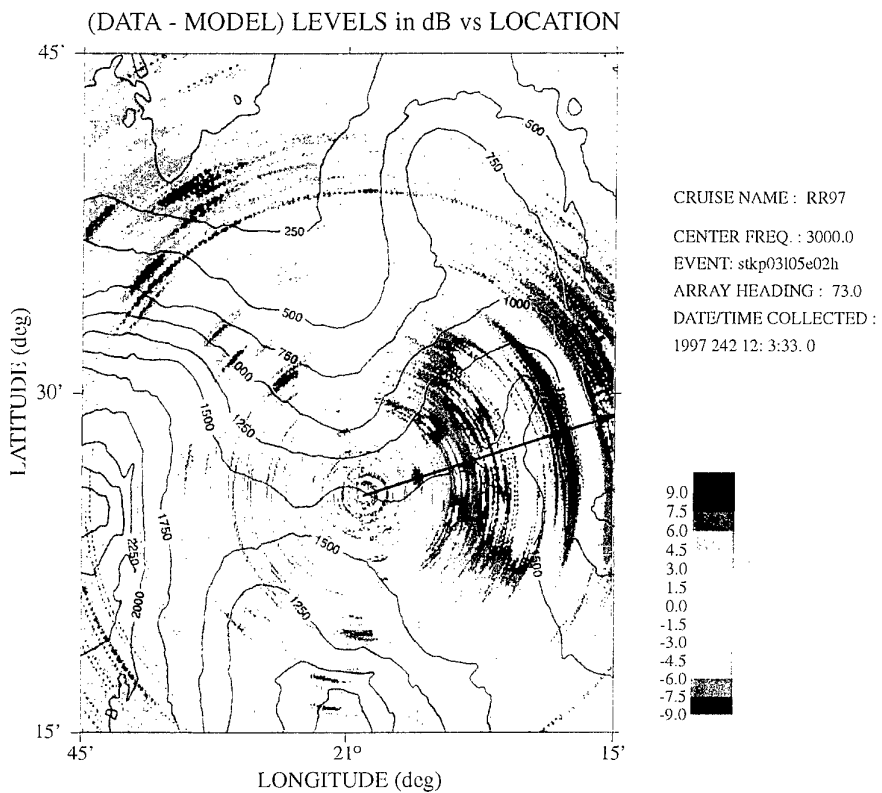


Figure 22 Scattering map (model-data differences) at 3000 Hz for Site KH.

Rapid Response '97 Reverberation Analysis
 MODEL-DATA COMPARISON AT SITE KH - 630 Hz
 Broadside beam, looking east-west

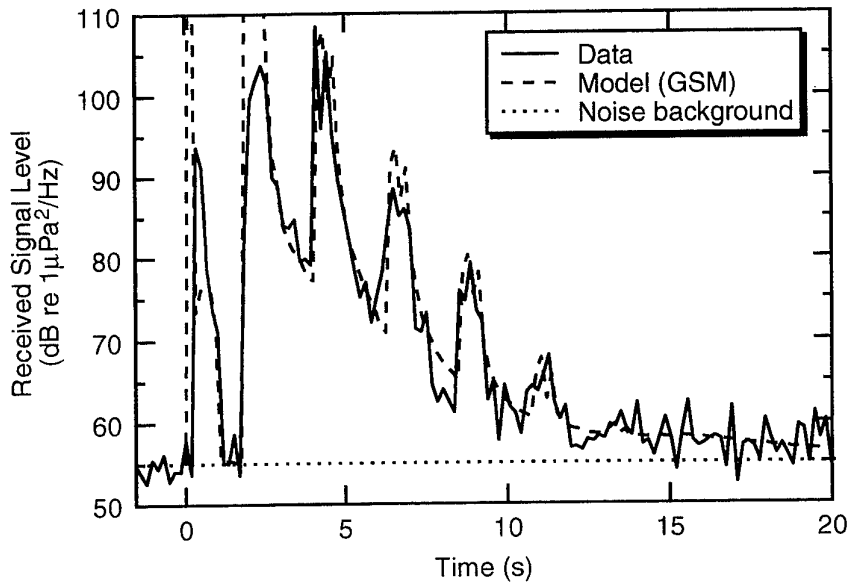


Figure 23 Model-data: line plot for site KH, at 630 Hz.

Rapid Response '97 Reverberation Analysis
 ESTIMATED BOTTOM LOSS
 Sites KD and KH

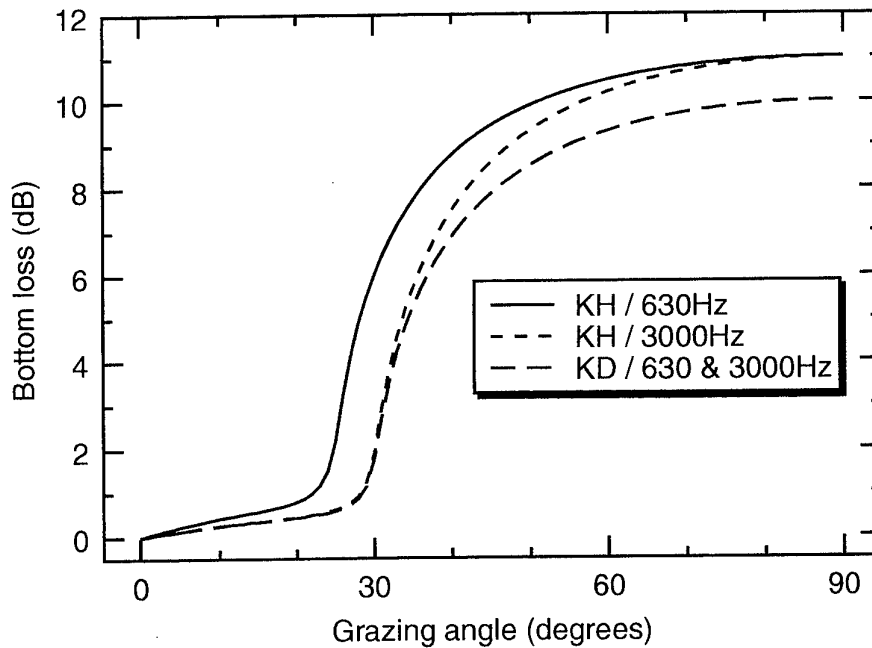


Figure 24 Bottom loss vs. grazing angle estimated for Sites KD and KH.

Rapid Response '97 Reverberation Analysis
 ESTIMATED BACKSCATTERING STRENGTHS
 Sites KD and KH

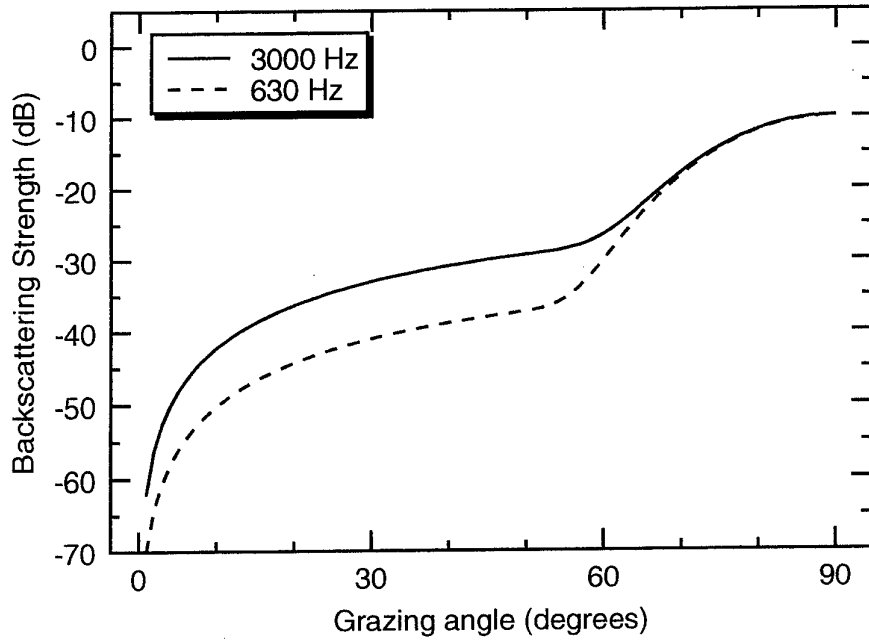


Figure 25 Backscattering strengths vs. grazing angle estimated for Sites KD and KH.

Rapid Response '97 Reverberation Analysis
 BOTTOM LOSS CURVES USED AT SITE IA
 (Data from Akal, extended to 90 degrees)

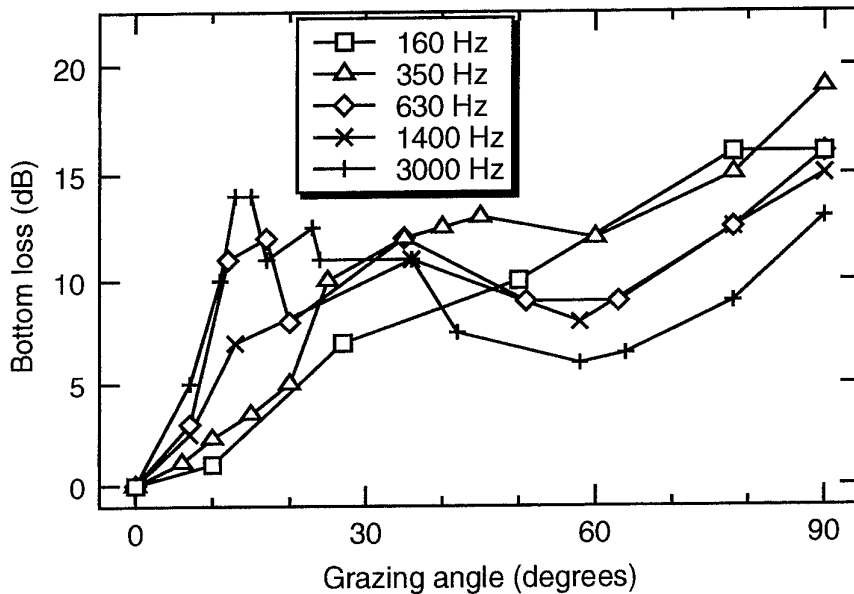


Figure 26 Bottom loss vs. grazing angle for Site IA.

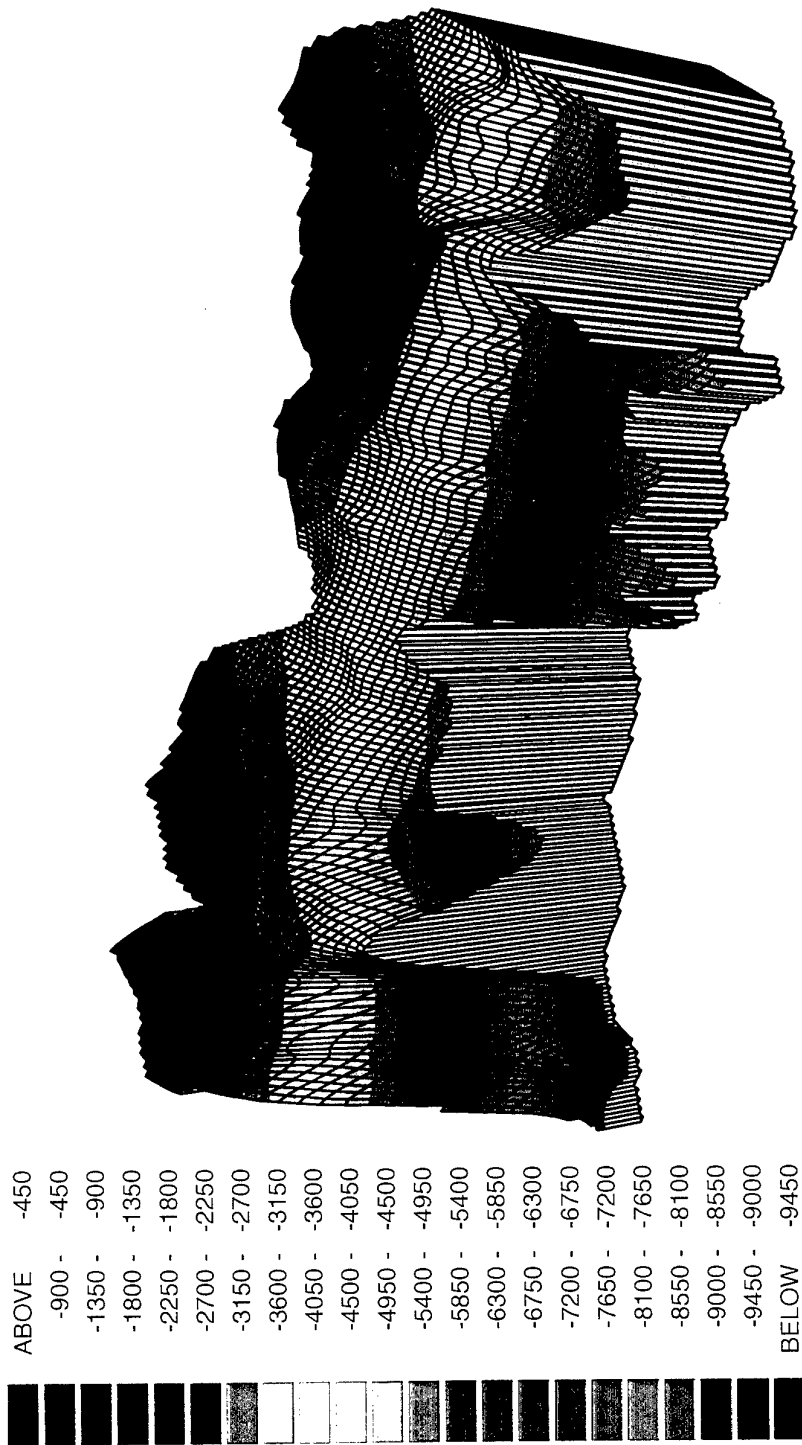


Figure 27 Swath mapping of regional escarpment west of Pilos.

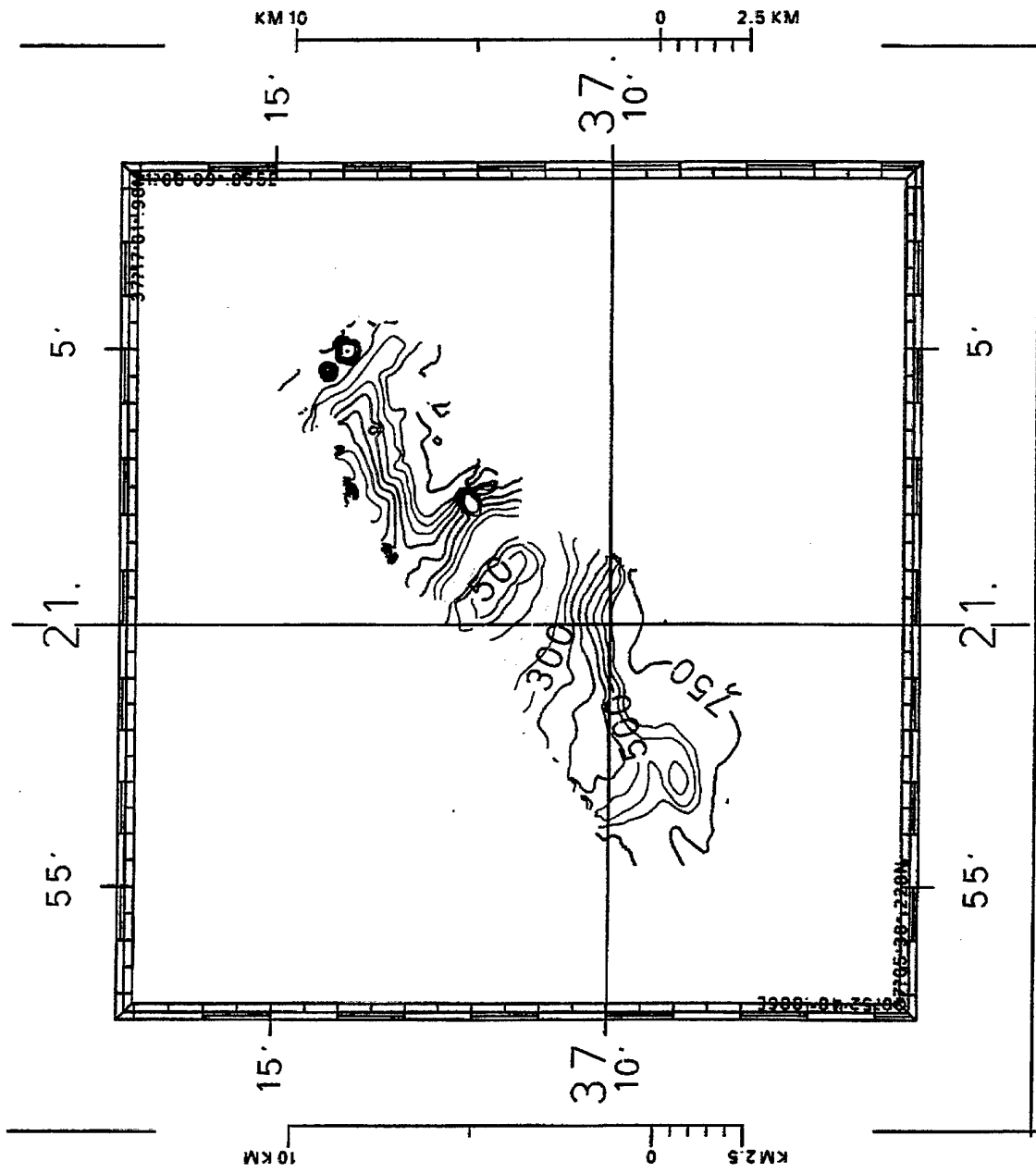


Figure 28 Bathymetric mapping of seamount south of Strophades Island.

Annex A Spectra for SUS charges

Table A-1 is a listing of spectral levels of SUS charges, from earlier SACLANTCEN measurements¹. The values at 3200 and 4032 Hz are extrapolated.

Table A-1 *Third-octave source spectral levels for 0.82 kg SUS charges at 3 depths.*

Frequency Hz	Source Level in dB re (1 ⁻² s at 1 m		
	17.3 m	87.0 m	243 m
12.5	203.02	205.47	199.33
15.7	210.36	209.11	200.45
19.8	207.81	211.92	201.80
25.0	208.09	212.78	203.65
31.5	206.95	210.01	205.81
39.7	205.84	210.20	207.90
50.0	205.03	207.80	209.55
63.0	205.33	207.22	208.77
79.4	204.51	203.59	204.53
100.0	203.89	205.44	206.28
126.0	203.02	203.95	202.38
158.7	201.76	201.98	204.34
200.0	200.76	201.27	202.01
252.0	199.61	200.33	199.97
317.5	198.12	199.12	198.58
400.0	196.53	197.71	198.45
504.0	194.61	196.39	196.79
635.0	193.05	195.28	195.63
800.0	192.38	194.16	194.63
1008.0	191.99	193.21	192.93
1270.0	190.59	191.05	190.78
1600.0	189.55	189.38	189.26
2015.9	188.25	187.27	186.92
2539.9	185.86	186.08	185.75
3200.	185.	184.	183.
4032.	184.	182.	181.

¹ T. Akal, Third-octave SUS spectra, Private communication, 1994.

Annex B Polygon tracks

The numbers in the following tables were noted in the hand-kept logs. The auto-logs will contain more accurate and more complete information. However, the information here may be useful in identifying many of the polar plots. Archival files (see Annex C) are often named with the following convention: where x is the polygon number, y is the leg number and z is the event number.

Table B-1 Summary of SUS drops for Polygon 1 (Site IA)

Leg	Event	SUS depth (m)	Water depth (m)	Ship heading (deg.)	Prakla array heading (deg.)	Prakla array depth (m)	Mid-Freq. array depth (m)
1	1	240	3299	007		249	
1	2	240	3219	351	357	253	
1	3	18	3252	352	357	252	
2	1	240	3233	222	214	331	
2	2	18	3224	222	214	322	
2	3	240	3337	221	214	320	
3	1	240	3238	070	070	248	
3	2	240	3270	068	070	245	
3	3	18	3259	069	070	243	
4	1	240	3295	285	289	331	
4	2	18	3269	286	289	324	
4	3	240	3279	286	287	319	
5	1	240	3272	146	142	253	
5	2	240	3269	146	142	253	
5	3	18	3312	146	141	255	

Table B-2 Summary of SUS drops for Polygon 2 (Site KD)

Leg	Event	SUS depth (m)	Water depth (m)	Ship heading (deg.)	Prakla array heading (deg.)	Prakla array depth (m)	Mid-Freq. array depth (m)
1	1	240	1220	216	215	110	96
1	2	240	1241	214	213	112	96
1	3	18	1253		212	112	98
1	4	18	1259		211		
2	1	240	1221	074	072	114	99
2	2	240	1206	074	070	116	
2	3	18	1183	076		116	
3	1	240	1178	284	285	117	99
3	2	240		284	286	118	98
3	3	18		283	285	118	97
4	1	240	1190	146	144	117	98
4	2	240		146	142	116	98
4	3	18	1163				
5	1	240	1176	351	357	116	96
5	2	240		353	354	116	98
5	3	18	1279	356	356	116	97

Table B-3 Summary of SUS drops for Polygon 3 (Site KH)

Leg	Event	SUS depth (m)	Water depth (m)	Ship heading (deg.)	Prakla array heading (deg.)	Prakla array depth (m)	Mid-Freq. array depth (m)
1	1	240	1730	288	287	121	78
1	2	240		294	286	127	
1	3	18			288		
2	1	240	1776	146	141	117	73
2	2	240	1635	142		118	
2	3	18		143	141	118	74
3	1	240	1635	353	354	121	76
3	2	240					
3	3	18					
4	1	240	1668	224	214	120	76
4	2	240			215	125	
4	3	18			213	122	76
5	1	240	1726	064	070	121	76
5	2	240					
5	3	18*					
		*all misfires					

Annex C Archival data

The raw data files are quite large (256 hydrophones sampled at 6000 Hz for several minutes). Even the processed data files were considered too large to be put on the Web Server, especially while at sea. A few examples may be on the **Rapid Response** 97 CD-ROM, with pointers to the files mentioned below.

The VLDS data tapes numbers were:

- for the Prakla array: 1266, 1269-72; 1275-79; 1283-87.
- for the mid-frequency array: 1267; 1273; 1274; 1280-81; 1282.

The HP optical disks numbers were:

- time series data (large files): 815-830, except 820 and 823.
- processed data: 820C (Side A).

The key processed data files are:

STK_Pkk_Lmm_Enn.DAT

ISO_Pkk_Lmm_Enn_c.DAT

- where *kk* is the polygon number 01, 02, or 03,
- mm* is the leg number 01 through 05,
- nn* is the event number 01, 02, 03,
- and *c* is a character (usually *l* or *h*, for high or low frequency).

Originals of figures from this report are available in the directory:
/usr3/users/preston/fromtape/rapr7rpt,
as PostScript files POST* or *.ps, where * indicates a wildcard.

ACKNOWLEDGEMENTS

The authors are indebted to Tuncay Akal for helping initiate the **Rapid Response** series of REA trials and Ron Wagstaff who pioneered this type of at-sea data collection and analysis in the 1980's. The authors acknowledge with gratitude the contributions made by the following people to the success of **Rapid Response 97**: John Osler and all the SACLANTCEN and *Alliance* sea-going personnel, with special mention to Piero Boni.

The Generic Sonar Model was made available by the U.S. Naval Underwater Warfare Centre. The ARL/PSU participation was funded by the U.S. Office of Naval Research Ocean Research Program.

Document Data Sheet

<i>Security Classification</i> UNCLASSIFIED		<i>Project No.</i> 01-A
<i>Document Serial No.</i> SR-280	<i>Date of Issue</i> August 2000	<i>Total Pages</i> 58 pp.
<i>Author(s)</i> Ellis, D., Preston, J. R., Hollett, R., Sellschopp, J.		
<i>Title</i> Analysis of towed array reverberation data from 160 to 4000 Hz during Rapid Response 97		
<i>Abstract</i> <p>This report describes reverberation measurements made during the NATO MILOC Rapid Environmental Assessment exercise Rapid Response 97, August-September 1997. SUS charges were used as sources and data were received on two arrays towed by R/V <i>Alliance</i>: the 256-hydrophone Prakla array and the 32-hydrophone mid-frequency array. The arrays were towed on five-leg tracks at three locations: a deep water site in the Ionian Sea and two sites in Kyparissiakos Gulf, a small intermediate-depth basin off the west coast of Greece.</p> <p>Reverberation data from the two arrays were analyzed in frequency bands from 160 Hz to 4000 Hz. Polar plots of the reverberation give a map of the prominent bottom-scattering features and provide a snapshot of the directional ambient noise field. Reverberation calculations were made using the Generic Sonar Model. A manual inversion procedure was used to estimate bottom loss and bottom backscattering. The model-data differences were used to produce scattering maps of the area. The polar plots and scattering maps indicated a number of scattering features not on the charts and identified a significant error in the charted position of an underwater escarpment to the south of Kyparissiakos Gulf. Follow-on swath mapping in two areas confirmed the results. The results illustrate the use of directional reverberation measurements as a useful remote sensing tool, for providing a rapid map of an unknown area and directing higher-resolution measurements in potentially interesting areas. The bottom loss and backscattering can be used in sonar models to provide improved performance predictions.</p>		
<i>Keywords</i> Rapid environmental assessment – Rapid Response – reverberation data – inversion – scattering strengths – bottom loss – Ionian Sea – Kyparissiakos Gulf		
<i>Issuing Organization</i> North Atlantic Treaty Organization SACLANT Undersea Research Centre Viale San Bartolomeo 400, 19138 La Spezia, Italy [From N. America: SACLANTCEN (New York) APO AE 09613]		 Tel: +39 0187 527 361 Fax: +39 0187 527 700 E-mail: library@saclantc.nato.int

The SACLANT Undersea Research Centre provides the Supreme Allied Commander Atlantic (SACLANT) with scientific and technical assistance under the terms of its NATO charter, which entered into force on 1 February 1963. Without prejudice to this main task - and under the policy direction of SACLANT - the Centre also renders scientific and technical assistance to the individual NATO nations.

This document is approved for public release.
Distribution is unlimited

SACLANT Undersea Research Centre
Viale San Bartolomeo 400
19138 San Bartolomeo (SP), Italy

tel: +39 0187 527 (1) or extension
fax: +39 0187 527 700

e-mail: library@saclantc.nato.int

NORTH ATLANTIC TREATY ORGANIZATION